NPS ARCHIVE
1999.03
TAN, H.

DUDLEY KNOX LIBRARY
NAVAL POSTGRADUATE SCHOOL
MONTEREY CA 93943-5101

# NAVAL POSTGRADUATE SCHOOL
## Monterey, California


# THESIS

**THE EFFECT OF ELEMENT MUTUAL COUPLING ON THE PERFORMANCE OF ADAPTIVE ARRAYS**

by

Tan Hong Wee

March 1999

Thesis Co-Advisors: Ramakrishna Janaswamy
David Jenn

**Approved for public release; distribution is unlimited.**

# REPORT DOCUMENTATION PAGE

*Form Approved*
*OMB No. 0704-0188*

Public reporting burden for this collection of information is estimated to average 1 hour per response, including the time for reviewing instruction, searching existing data sources, gathering and maintaining the data needed, and completing and reviewing the collection of information. Send comments regarding this burden estimate or any other aspect of this collection of information, including suggestions for reducing this burden, to Washington headquarters Services, Directorate for Information Operations and Reports, 1215 Jefferson Davis Highway, Suite 1204, Arlington, VA 22202-4302, and to the Office of Management and Budget, Paperwork Reduction Project (0704-0188) Washington DC 20503.

| 1. AGENCY USE ONLY *(Leave blank)* | 2. REPORT DATE | 3. REPORT TYPE AND DATES COVERED |
|---|---|---|
| | March 1999 | Master's Thesis |

**4. TITLE AND SUBTITLE**
**The Effect of Element Mutual Coupling on the Performance of Adaptive Arrays**

**5. FUNDING NUMBERS**

**6. AUTHOR(S)**
Hong Wee, Tan

**7. PERFORMING ORGANIZATION NAME(S) AND ADDRESS(ES)**
Naval Postgraduate School
Monterey, CA 93943

**8. PERFORMING ORGANIZATION REPORT NUMBER**

**9. SPONSORING / MONITORING AGENCY NAME(S) AND ADDRESS(ES)**

**10. SPONSORING / MONITORING AGENCY REPORT NUMBER**

**11. SUPPLEMENTARY NOTES**
The views expressed in this thesis are those of the author and do not reflect the official policy or position of the Department of Defense or the U.S. Government.

**12a. DISTRIBUTION / AVAILABILITY STATEMENT**
Approved for public release; distribution is unlimited.

**12b. DISTRIBUTION CODE**

**13. ABSTRACT *(maximum 200 words)***

Adaptive arrays are highly versatile sensors employed in modern wireless communication systems to combat interference and multi-path fading and thereby increase system capacity. In adaptive processing, weights are attached to the incoming signal at each element to produce nulls in the directions of interferers. However, mutual coupling is normally ignored in such processing. Instead, the principle of pattern multiplication is used, where the assumption is that the radiation pattern of an array is the individual radiation pattern of the elements multiplied by an array factor. This assumption ignores mutual coupling and the error can be significant under certain conditions. This work begins by setting up the scenario of an adaptive array in a mobile communications scenario in a scattering environment. Following that, we introduce the theories of mutual coupling and beam-forming. Expressions for the optimum solutions and the signal-to-interference-plus-noise ratio are then derived based on the preceding discussions. Subsequently, we show the effects of mutual coupling and the conditions under which the effect is significant. In addition, we will examine various parameters involved in our scenario and how they affect the performance of the adaptive array.

**14. SUBJECT TERMS**
Adaptive arrays, mutual coupling, mobile communications

**14. NUMBER OF PAGES**
68

**15. PRICE CODE**

| 17. SECURITY CLASSIFICATION OF REPORT | 18. SECURITY CLASSIFICATION OF THIS PAGE | 19. SECURITY CLASSIFI- CATION OF ABSTRACT | 20. LIMITATION OF ABSTRACT |
|---|---|---|---|
| Unclassified | Unclassified | Unclassified | UL |

NSN 7540-01-280-5500

Standard Form 298 (Rev. 2-89)
Prescribed by ANSI Std. 239-18

DUDLEY KNOX LIBRARY
NAVAL POSTGRADUATE SCHOOL
MONTEREY, CA 93943-5101

Approved for public release; distribution is unlimited

# THE EFFECT OF ELEMENT MUTUAL COUPLING ON THE PERFORMANCE OF ADAPTIVE ARRAYS

Tan, Hong Wee
Major, Republic of Singapore Navy
B.A., Cambridge University, England, 1990
M.A., Cambridge University, England, 1994

Submitted in partial fulfillment of the
requirements for the degree of

**MASTER OF SCIENCE IN SYSTEMS ENGINEERING**

from the

**NAVAL POSTGRADUATE SCHOOL**
**March 1999**

DUDLEY KNOX LIBRARY
NAVAL POSTGRADUATE SCHOOL
MONTEREY CA 93943-5101

## ABSTRACT

Adaptive arrays are highly versatile sensors employed in modern wireless communication systems to combat interference and multi-path fading and thereby increase system capacity. In adaptive processing, weights are attached to the incoming signal at each element to produce nulls in the directions of interferers. However, mutual coupling is normally ignored in such processing. Instead, the principle of pattern multiplication is used, where the assumption is that the radiation pattern of an array is the individual radiation pattern of the elements multiplied by an array factor. This assumption ignores mutual coupling and the error can be significant under certain conditions. This work begins by setting up the scenario of an adaptive array in a mobile communications scenario in a scattering environment. Following that, we introduce the theories of mutual coupling and beam-forming. Expressions for the optimum solutions and the signal-to-interference-plus-noise ratio are then derived based on the preceding discussions. Subsequently, we show the effects of mutual coupling and the conditions under which the effect is significant. In addition, we will examine various parameters involved in our scenario and how they affect the performance of the adaptive array.

## TABLE OF CONTENTS

## LIST OF FIGURES

## LIST OF TABLES

## ACKNOWLEDGEMEMT

The author would like to express his sincere gratitude to Dr Ramakrishna Janaswamy and Dr David Jenn at the Naval Postgraduate School, both of whom have made invaluable contribution to the completion of this work. And to my wife Sharon, for her telepathic support throughout.

# I. INTRODUCTION

Array antennas are well known for their versatility in many areas, not least of which in point-to-point communication. By a process of beam-forming, an array antenna can steer its main beam in the direction of its intended transmitter or receiver while simultaneously pointing its nulls to cancel interference sources. Furthermore, adaptive algorithms have been introduced [Ref. 1 : p586 - 591] to infer and respond to the directions of these (desired and interference) sources, the positions of which change with time. There is currently a lot of interest in using adaptive antennas in mobile communications to increase systems capacity or reduce interference.

However, the effect of mutual coupling has received little attention in the adaptive array processing community. It is often assumed that the beam pattern of an array is the individual pattern of an element multiplied by an array factor, in which mutual coupling is ignored. In this work, we will show that this error is significant under certain conditions and examine the effect mutual coupling has on the performance of array antennas.

We begin in Chapter II by describing the scenario of mobile communications on which this work is based, followed by theoretical discussions on mutual coupling and beam-forming. Finally, we shall derive useful expressions for optimum adaptive solutions and for the signal-to-interference-plus-noise ratio (SINR), which will serve as the yardstick for measuring the performance of an array antenna.

In Chapter III, we will show the effect of mutual coupling and the conditions under which this effect is significant. In addition, we will examine various parameters involved in our scenario and how they affect the performance of the adaptive array.

## II. THEORY

In this work we will look at the effect of element mutual coupling on the signal-to-interference-plus-noise ratio (SINR) of an adaptive array whose design is based on the minimum mean square error algorithm. The elements of the array are assumed to be dipoles and the analysis will be carried out in terms of the array mutual impedance. A variable number of sources of interference as well as variable inter-element spacing will be considered in the study.

### A. DESCRIPTION OF THE PROBLEM

We consider the case of K+1 transmitters (one desired and K interference) all radiating narrowband signals to a receiver at the same carrier frequency. The scenario is illustrated in Fig 2.1. The transmitters (also referred to as sources) are all embedded in a scattering environment. The scatterers, which could represent reflecting obstacles surrounding the source, are assumed to be distributed uniformly around each source over a circular region of radius $r_k$. We assume single bounce scattering of waves, meaning that waves reach the receiver via single scattering off the obstacles. We further assume a 2D situation where waves travel only in the azimuthal (horizontal) plane. Because of the presence of scatterers, waves will not arrive just from a single direction for each source but from an angular region determined by $r_k$ and the distance $R_k$ between the $k^{th}$ source and the receiver. The receiving antenna is assumed to be an N-element linear array with an inter-element spacing d. The elements are assumed to be center-fed half wave dipoles oriented along the z axis, so the pattern of an isolated element in the azimuth plane is constant. The mean directions of the desired source (k=0) and the $k^{th}$ interferer (k=1 to K)

are denoted by $\bar{\phi}_o$ and $\bar{\phi}_k$ respectively. Let $\phi_k$ be the angle from any scatterer around the $k^{th}$ source to the array and $\alpha_k = \phi_k - \bar{\phi}_k$, as shown. The angle of arrival $\alpha_k$ is then measured from the mean direction $\bar{\phi}_k$ for each source.

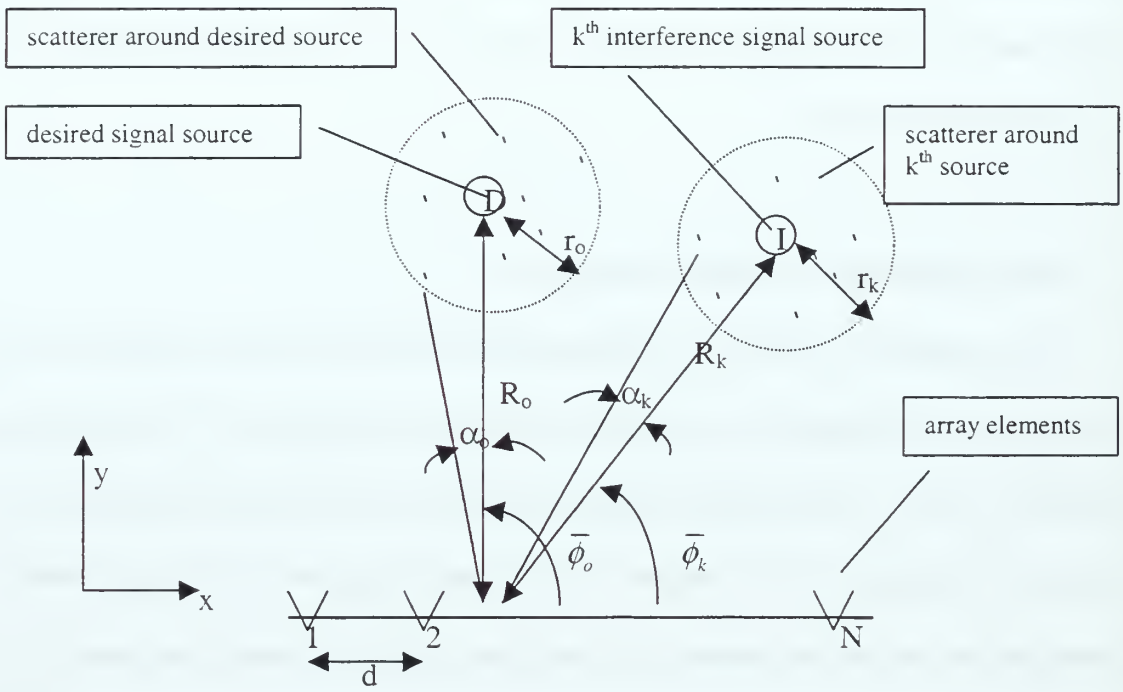


Fig 2.1 Wireless Communication Scenario

Because of the multi-path phenomenon, the amplitude, phase and angle of arrival of waves from each source will be random variables. The interferers are assumed to be arbitrarily located about the receiver. The purpose of the array is two-fold:

i) the array weights are chosen to produce nulls in the direction of the interferers, and thereby reduce their influence on the received signal, and

ii) if $N > K+1$, to provide diversity gain against multi-path fading.

The weights of the array are continually changed depending on the location of the interferers. Such an array is termed as *adaptive array* or *smart antenna*. The situation considered above may well pertain to the case of wireless network in a tactical battlefield or to the case of mobile cellular radio where K+1 co-channel mobiles send signals to a base-station receiver. We have assumed thus far that the mean directions of the desired source and the interferers are known *a priori*. This is seldom the case in reality. In a practical mobile situation, the sources move around in space and their directions are not known precisely. In such a case, the weights are determined by means of either the Least Mean Square (LMS) or Recursive Least Square (RLS) algorithm. However the present case is still of interest in applications such as wireless local loops where wireless service is provided to fixed subscribers and the directions of subscribers available from a previously compiled data base.

Since the calculation of optimum weights requires the covariance matrix of the received signal vector, we would like to know the probability density function (pdf) of the angle of arrival. For a uniform density of scatterers about the source, the pdf of the angle of arrival with respect to the mean direction is given as [Ref. 2 : p24-25] :

$$p(\alpha_k) = \frac{2b_k}{\pi} \cos\alpha_k \sqrt{1 - b_k^2 \sin^2 \alpha_k} \qquad |\alpha_k| \le \zeta_k \qquad (1)$$

where $b_k = R_k / r_k$ (2)

and $\zeta_k$ is the maximum angle of arrival from the $k^{th}$ scattering region, given by

$$b_k \sin\zeta_k = 1$$

For subsequent analysis, it is simpler to express the pdf in terms of a new angle $\gamma_k$ defined by $\sin\gamma_k = b_k \sin\alpha_k$ ; then

$$\cos\gamma_k \, d\gamma_k = b_k \cos\alpha_k \, d\alpha_k \tag{3}$$

Using this transformation of variable [Ref. 3 : p122], the pdf of $\gamma_k$ is:

$$p(\gamma_k) = p(\alpha_k) \left| \frac{d\alpha_k}{d\gamma_k} \right|$$

$$= \frac{2}{\pi} \cos^2 \gamma_k \qquad -\frac{\pi}{2} \le \gamma_k \le \frac{\pi}{2} \tag{4}$$

This will be applied in Section 1D when the expressions for optimum weights and SINR are derived.

The mean value of $\alpha_k$ is $\overline{\alpha}_k = 0$ and its variance $\tilde{\alpha}_k^2$ for $b_k >> 1$ is approximately given as [Ref. 4] :

$$\tilde{\alpha}_k^2 = \zeta_k^2 - \frac{3}{4b_k^2} \tag{5}$$

$$\approx \left( \frac{1}{2b_k} \right)^2 \approx \left( \frac{\zeta_k}{2} \right)^2$$

The root mean square (rms) value of the angular spread is then $\frac{\zeta_k}{2}$. For example, with $r_k$ = 100 m and $R_k$ = 1 km, $\zeta_k = 5.7^\circ$ and $\tilde{\alpha}_k = 2.85^\circ$.

## B. MUTUAL COUPLING

In an array of electrically identical antenna elements, it is common to assume the total radiation pattern to be the product of the array factor and the radiation pattern of the individual elements, i.e., total radiation pattern = (array factor) x (element radiation pattern). Implicit in this formulation is the assumption that the individual radiation

patterns remain the same even when placed in proximity of each other when mutual electromagnetic interaction exists. However, such an assumption is erroneous in view of element mutual coupling. When an antenna array is designed to provide diversity gain, mutual coupling will disturb the spatial correlation of signals received by the array. In this thesis, we will examine the effect of mutual coupling on the performance of the array.

The input impedance of an isolated antenna is simply the ratio of the voltage applied (at its terminals) to the resulting terminal current. This is known as the self-impedance and is, in general, a complex value as both voltage and current are of different phases. When two antennas are located in close proximity, the current distribution (and hence the radiation pattern) on one is affected by the field radiated from the other. This is known as mutual coupling. To account for the mutual coupling effect, extra impedance terms called mutual impedances are needed.

In general, the solution to the mutual impedance for dipoles can be accomplished by way of coupled integral equations. Apart from its dependence on physical dimensions and separation distance between the elements, the mutual impedance also changes with the number of antenna elements. For an array of N elements, the impedance matrix can be written as $Z_{mn}^{[N]}$, denoting the mutual impedance on the $m^{th}$ element induced by the $n^{th}$ element in an N-element array. The details of mutual impedance calculation are not within the scope of this paper; we are interested in the effects it has on array antennas. We will use results from simulation programs or from analytical expressions. As mentioned earlier, for the sake of simplicity, we shall only concern ourselves with half wavelength dipoles of small thickness. Even though $Z_{mn}^{[N]}$ varies with N, we will assume $Z_{mn}^{[N]} \approx Z_{mn}^{[2]}$; actual computation of $Z_{mn}^{[4]}$ and $Z_{mn}^{[8]}$ show them to be very close to $Z_{mn}^{[2]}$. (The

superscript [2] is subsequently dropped.) $Z_{mn}$, the mutual impedance between two side-by-side dipoles, each of length L and separated by a distance d, is given by [Ref. 5: p265] :

$$Z_{12} = 30\{2E_i(-jk_o d) - E_i[-jk_o(\sqrt{d^2 + L^2} + L)] - E_i[-jk_o(\sqrt{d^2 + L^2} - L)]\} \quad (6)$$

where $k_o = 2\pi/\lambda$ is the wavenumber in free space, and

$E_i(\pm jy) = C_i(y) \pm j\, S_i(y)$

$C_i(y)$ = cosine integral

$S_i(y)$ = sine integral

It is obvious that the inter-element spacing d has an influence on $Z_{mn}$; as the distance apart increases, one can expect the contribution from other array elements to be reduced and hence $Z_{mn}$ ($m \neq n$) diminishes. The resultant impedance matrix **Z** is then almost diagonal and mutual coupling can be ignored.

## C. BEAM-FORMING ALGORITHM

Consider an arrangement of N elements spaced d apart (Fig 2.2). An electromagnetic wave arriving from bearing $\phi$ induces an open circuited voltage $V_n^{oc}$ on the $n^{th}$ element. The open circuited voltage depends on the incident field and the orientation of the dipoles with respect to the incoming wave. The coupling between the elements is governed by the impedance matrix **Z**. It is assumed that the adaptive processor presents load impedance $(Z_L)_n$ (n=1, 2, ... N) at each element. The terminal voltage and current at the $n^{th}$ port are denoted by $V_n$ and $I_n$ respectively. It is clear that $\mathbf{V} = -\mathbf{Z_L I}$, where **V** is a vector of voltages presented to the adaptive processor and $\mathbf{Z_L}$ is the diagonal matrix = diag($Z_{L1}$ , $Z_{L2}$ , ... , $Z_{LN}$).

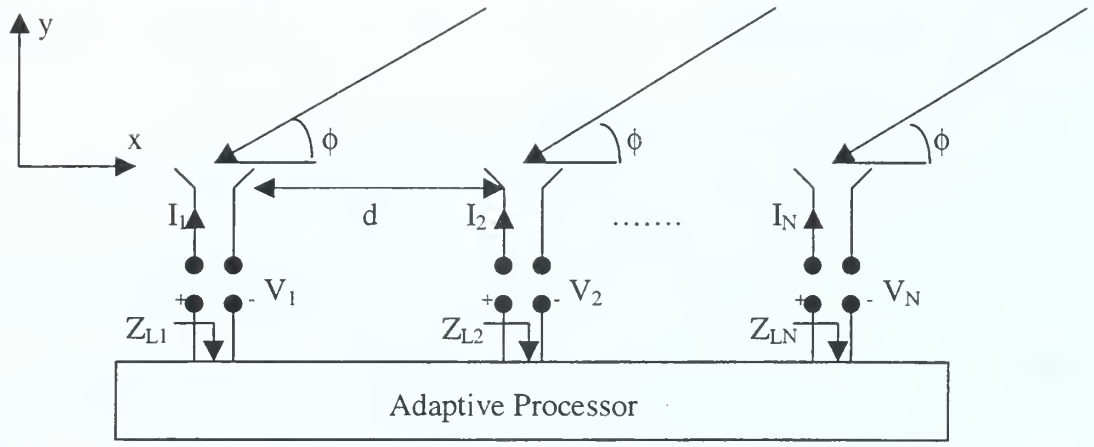


Fig 2.2 Array of N elements

The terminal voltage is related to the open circuited voltage by means of the impedance matrix as :

$$V_1 = Z_{11}I_1 + Z_{12}I_2 + Z_{13}I_3 + \ldots + Z_{1N}I_N + V_1^{oc}$$

$$V_2 = Z_{21}I_1 + Z_{22}I_2 + Z_{23}I_3 + \ldots + Z_{2N}I_N + V_2^{oc}$$

$$V_3 = Z_{31}I_1 + Z_{32}I_2 + Z_{33}I_3 + \ldots + Z_{3N}I_N + V_3^{oc}$$

$$\vdots \qquad \vdots \qquad \vdots$$

$$\vdots \qquad \vdots \qquad \vdots$$

$$V_N = Z_{N1}I_1 + Z_{N2}I_2 + Z_{N3}I_3 + \ldots + Z_{NN}I_N + V_N^{oc}$$

or equivalently,

$$\mathbf{V} = \mathbf{ZI} + \mathbf{V}^{oc} \qquad (7)$$

For a dipole antenna the open circuited voltage can be obtained from the effective length of the antenna by

$$V_n^{oc} = \bar{h} \bullet \bar{E}_n^{inc} \tag{8}$$

where $\bar{h}$ = vector effective length of $n^{th}$ element

$\bar{E}_n^{inc}$ = incident electric field on $n^{th}$ element.

For dipoles of length L, oriented along the z-axis and having a sinusoidal distribution $I(z) = I_o \sin\{k_o(L/2-|z|)\}$, the effective length is

$$\bar{h} = \hat{\theta}\frac{\lambda}{\pi}\frac{f(\theta)}{\sin(\frac{k_o L}{2})} \tag{9}$$

where $\theta$ is the usual polar coordinate in the spherical coordinate system and

$$f(\theta) = \frac{\cos(\frac{k_o L}{2}\cos\theta) - \cos(\frac{k_o L}{2})}{\sin\theta}$$

is the radiation pattern of the dipole.

The electric field incident on the $n^{th}$ dipole is of the form,

$$\bar{E}_n^{inc} = \hat{\theta} E_o e^{jk_o d(n-1)\cos\phi}$$

In the present case, $\theta = \pi/2$ and the radiation pattern of the dipole reduces to

$$f(\theta) = (1 - \cos\frac{k_o L}{2})$$

$$\text{Therefore, } V_n^{oc} = \frac{\lambda}{\pi} E_o \frac{1-\cos(\frac{k_o L}{2})}{\sin(\frac{k_o L}{2})} e^{jk_o d(n-1)\cos\phi} = V_o e^{jk_o d(n-1)\cos\phi} \tag{10}$$

where $V_o = \frac{\lambda E_o}{\pi}\tan(\frac{k_o L}{4})$

Using (10) in (7) and substituting $\mathbf{V} = -\mathbf{Z_L I}$, we get

$$\mathbf{V} = \mathbf{Z_c V^{oc}} \tag{11}$$

where $\mathbf{Z_c = Z_L Z_o^{-1}}$ (12)

and $\mathbf{Z_o = (Z_L + Z)}$ (13)

It is this voltage vector **V** and not $\mathbf{V^{oc}}$ that is available for array processing. It is seen that the effect of mutual coupling is to couple the open circuited voltages induced at each element. Thus mutual coupling will affect the spatial correlation between the element signals and hence affect the diversity gain of the antenna.

In the presence of thermal noise, the total voltage input to the adaptive processor is

$$\mathbf{V_t = Z_c V^{oc} + N(t)} \quad (14)$$

where **N**(t) = column vector of thermal noise.

With this input signal vector $\mathbf{V_t}$, the adaptive processor attaches a weight $w_n^*$ (* is the complex conjugate operator) to each $(V_t)_n$ as shown in Fig 2.3, and produces a combined output $S_r$.

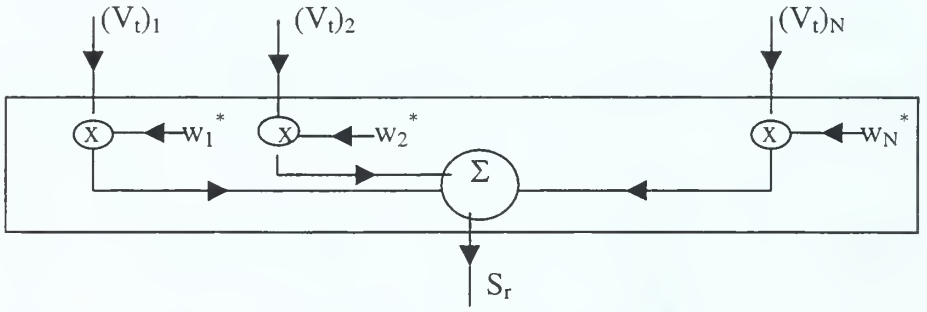


Fig 2.3 Adaptive Processor

In mathematical terms, the array response is

$$S_r = w_1^* V_1 + w_2^* V_2 + .... + w_N^* V_N$$

$$= \mathbf{w^H V_t} \quad (15)$$

where $^{H}$ denotes the Hermitian operator (transpose and conjugate).

By varying the weighting vector **w**, up to N-1 nulls can be steered in any direction. For example, in the absence of mutual coupling and scattering, and using a 4-element array, if the nulls are desired at $\phi_1$ , $\phi_2$ and $\phi_3$ we choose the weights according to

$$\begin{pmatrix} V_1 & V_1^2 & V_1^3 \\ V_2 & V_2^2 & V_2^3 \\ V_3 & V_3^2 & V_3^3 \end{pmatrix} \begin{pmatrix} \frac{w_2}{w_1} \\ \frac{w_3}{w_1} \\ \frac{w_4}{w_1} \end{pmatrix} = \begin{pmatrix} -1 \\ -1 \\ -1 \end{pmatrix} \tag{16}$$

where $V_k = e^{-jk_o d(n-1)\cos\phi_k}$ , k = 1,2,3. For $\phi_1 = 45^\circ$, $\phi_2 = 90^\circ$, $\phi_3 = 135^\circ$ and $d = \lambda/2$, we get $\frac{w_2}{w_1} = 0.2114$, $\frac{w_3}{w_1} = -0.2114$ and $\frac{w_4}{w_1} = 1$. The array response to a plane wave arriving from angle $\phi$ is plotted in Fig 2.4.

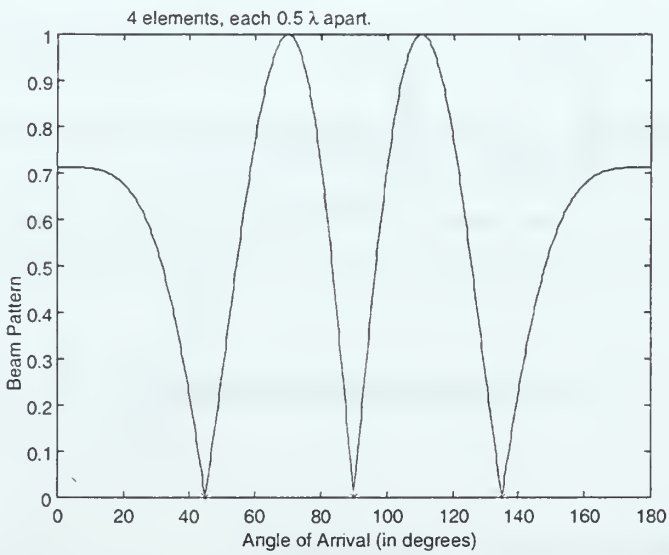


Fig 2.4 Beam pattern of a 4 element array, intended nulls at $\phi = 45^\circ$, $90^\circ$ and $135^\circ$

### 1. Criteria for Optimum Weight

It was shown in the preceding paragraphs that, by using an appropriate weighting vector, one is able to direct the nulls towards the direction of interference sources, thereby cancelling them out. How does one choose the weights in the presence of noise and scatterers?

The choice of the weighting function is based on the statistics of the total signal received (desired + interference). Basically, the objective is to optimize the beam towards the desired signal according to a prescribed criterion, of which there are several. It has been shown [Ref. 5: p41] that the various criteria (including the Minimum Mean Square Error (MMSE) and the Maximum SINR criteria) converge to the same Wiener solution, differing only by a trivial scalar factor. Since the solutions are all the same, we shall use the MMSE criterion. In the MMSE algorithm, the weights are chosen to minimize the error, defined as:

$$\text{error} = < | A_r(t) - S_r(t) |^2 > \qquad (17)$$

where $< >$ is the expectation operator. The weights that minimize the error are shown to be of the form [Ref. 6: p39] :

$$\mathbf{w_{opt}} = \Phi^{-1} \mathbf{S} \qquad (18)$$

where

$$\Phi = \text{covariance matrix} = <\mathbf{V_t}\, \mathbf{V_t}^{\mathbf{H}}> \qquad (19)$$

$$\mathbf{S} = <\mathbf{A_r}^{\mathbf{H}}\, \mathbf{V_t}> \qquad (20)$$

$$A_r = \text{reference signal} = a_o \exp[j(\omega t + \beta_o)]$$

## 2. Choice of inter-element spacing d

Before proceeding to the calculation of the weight vectors, it would be instructive to consider the effect the separation distance between array elements on the input signal. Suppose there were no mutual coupling, no thermal noise (**N**(t)=0) and all loads are identical (hence $\mathbf{Z_c} = z_c\mathbf{U}$ , where **U** is an NxN identity matrix and $z_c = \frac{Z_L}{Z_L + Z_{11}}$). Then using (10) - (14), the input signal to the array processor is :

$$(\mathbf{V}_t)_n = z_c V_o e^{jk_o d(n-1)\cos\phi} \tag{21}$$

Suppose the weights are all equal, i.e. $w_n = w$ for all n, then

$$\begin{aligned} S_r(\phi) &= \sum_1^N w_n * V_n \\ &= w * z_c V_o \sum_1^N e^{jk_o d(n-1)\cos\phi} \\ &= w * z_c V_o \frac{1 - e^{jNk_o d\cos\phi}}{1 - e^{jk_o d\cos\phi}} \end{aligned} \tag{22}$$

The maxima are obtained at $\cos\phi = \pm n(\frac{\lambda}{d})$, (n=0,1,2...) where the denominator becomes zero. In general, there is the desired major lobe and other major lobes called grating lobes. To avoid these grating lobes, one chooses $\frac{\lambda}{d} > 1$, so that the above equation will have only one maximum corresponding to n=0. Therefore in this paper, we shall be primarily considering values of d up to $1\lambda$ for most results.

The nulls of $S_r(\phi)$ occur when the numerator alone goes to zero, i.e., whenever $e^{jNk_o d\cos\phi} = 1$, assuming $k\,d\cos\phi \neq 2\pi n$. This means $\cos\phi = \pm m(\frac{\lambda}{Nd})$, where m is any integer. As such, for $\frac{\lambda}{d} < 1$, there are several solutions for $\phi$ and m, which implies the presence of multiple nulls, which might dramatically affect the SINR if they coincide with the direction of the desired source. The above example assumed equal weights and the absence of noise and mutual coupling. If these were taken into consideration, the extra lobes would, in general still be present, albeit shifted.

## D. EXPRESSIONS FOR $W_{opt}$ AND SINR

With the results of the first three sections, we are now ready to proceed to derive the expressions for the optimum weighting vector ($\mathbf{w_{opt}}$) and the signal-to-interference-plus-noise ratio (SINR).

To begin with, let the desired signal be of the form $A_o(t)\ \mathbf{V_o}^{oc}$ and the interference signal be of the form $A_k(t)\ \mathbf{V_k}^{oc}$ where

$$A_o(t) = a_o \exp[j(\omega t + \beta_o)] \qquad (23)$$

$$A_k(t) = a_k \exp[j(\omega t + \beta_k)] \qquad (24)$$

$$(\mathbf{V_o}^{oc})_n = V_o \exp[j(k_o\, d\, (n-1) \cos\phi_o)] \qquad (25)$$

$$(\mathbf{V_k}^{oc})_n = V_o \exp[j(k_o\, d\, (n-1) \cos\phi_k)] \qquad (26)$$

$a_o$ , $a_k$ = amplitudes of signals

$\beta_o$ , $\beta_k$ = phases of signals

Then the input signal to the adaptive processor is

$$\mathbf{V_t = Z_c\, V^{oc} + N(t)}$$

$$= \mathbf{Z_c}\,(A_o\, \mathbf{V_o^{oc}} + \sum_{k=1}^{K} A_k\, \mathbf{V_k^{oc}}) + \mathbf{N(t)} \qquad (27)$$

1. **Optimum Weight $\mathbf{w_{opt}}$**

We now attempt to find a convenient expression for the covariance matrix $\Phi$. Using equation (19) :

$$\Phi = \langle \mathbf{V_t\, V_t^H} \rangle$$

$$= \langle (\mathbf{Z_c\, V^{oc} + N})\, (\mathbf{Z_c\, V^{oc} + N})^{\mathbf{H}} \rangle$$

$$= \mathbf{Z_c} \langle \mathbf{V^{oc}\, V^{oc\,H}} \rangle \mathbf{Z_c^H} + \langle \mathbf{N\, V^{oc\,H}} \rangle \mathbf{Z_c^H}$$

$$+ \mathbf{Z_c} \langle \mathbf{V^{oc}\, N^H} \rangle + \langle \mathbf{N\, N^H} \rangle$$

The following assumptions are made :

i) The noise voltage at each port is independent of the each other and of the signals; its pdf is assumed to be zero mean Gaussian.

ii) The open circuited desired signal is assumed to be independent of the open circuited interfering signals.

iii) The open circuited interfering signals are assumed to be independent of one another.

iv) The amplitude, phase and angle of arrival of the signal from each source vary independently of each other.

It is shown in Appendix A that this eventually reduces to :

$$\Phi = \tilde{V}_N^2 + \tilde{V}_N^2\, \mathbf{Z_c}\, \xi_o\, \mathbf{C_o\, Z_c^H} + \tilde{V}_N^2\, \mathbf{Z_c}\, \Sigma\, \xi_k\, \mathbf{C_k\, Z_c^H}$$

$$= \tilde{V}_N^2\, [\, \mathbf{U} + \mathbf{Z_c}\, \xi_o\, \mathbf{C_o\, Z_c^H} + \mathbf{Z_c}\, \Sigma\, \xi_k\, \mathbf{C_k\, Z_c^H}\, ] \qquad (28)$$

where $\tilde{V}_N^2$ = mean square noise voltage at each port

**U** is the N x N identity matrix

$\mathbf{Z_c}$ = as defined in eqn (12)

$$[\mathbf{C_k}]_{mn} = e^{jk_o d(m-n)\cos\bar{\phi}_k} \frac{2J_1\left(\frac{k_o d(m-n)\sin\bar{\phi}_k r_k}{R_k}\right)}{\frac{k_o d(m-n)\sin\bar{\phi}_k r_k}{R_k}}, \quad k = 0,1,2,\ldots K \qquad (29)$$

$\xi_o$ = input signal (desired source) to thermal noise ratio = $\dfrac{V_o^2 < a_d^2 >}{\tilde{V}_N^2}$

$\xi_k$ = input interference ($k^{th}$ interfering source) to thermal noise ratio = $\dfrac{V_o^2 < a_k^2 >}{\tilde{V}_N^2}$

$J_1$ (.) = Bessel's function of the first kind of order one

It is also shown in Appendix A that :

$$\mathbf{S} = \langle A_r^* \mathbf{V_t} \rangle$$

$$= \tilde{V}_N^2 \xi_o \mathbf{Z_c} \mathbf{C_s} \qquad (30)$$

where

$$[C_s]_m = e^{jk_o d(m-1)\cos\phi_o} \frac{2J_1\left(\frac{k_o d(m-1)\sin\bar{\phi}_o r_o}{R_o}\right)}{\frac{k_o d(m-1)\sin\bar{\phi}_o r_o}{R_o}} \qquad (31)$$

Substituting eqns (30) and (31) into eqn (18) :

$$\mathbf{w_{opt}} = \Phi^{-1} \mathbf{S}$$

$$= a_o \xi_o [\mathbf{U} + \mathbf{Z_c} \xi_o \mathbf{C_o} \mathbf{Z_c}^{\mathbf{H}} + \mathbf{Z_c} \Sigma \xi_k \mathbf{C_k} \mathbf{Z_c}^{\mathbf{H}}]^{-1} \mathbf{Z_c} \mathbf{C_s} \qquad (32)$$

where $a_o \xi_o$ is a trivial constant factor and is subsequently dropped.

## 2. Signal-to-Interference-Plus-Noise Ratio

With the weight thus calculated, we can proceed to evaluate the SINR, which gives a measure of the effectiveness of the array :

$$\text{SINR} = \frac{\text{Power Received from desired signal}}{\text{Noise Power + Interference Power}}$$

$$= \frac{P_o}{P_N + \sum_{k=1}^{K} P_k} \tag{33}$$

where, from Appendix B,

$$P_o = < (\mathbf{w}^H \mathbf{Z}_c A_o \mathbf{V}_o^{oc}) (\mathbf{w}^H \mathbf{Z}_c A_o \mathbf{V}_o^{oc})^H >$$

$$= \tilde{V}_N^2 \xi_o \mathbf{w}^H \mathbf{Z}_c \mathbf{C}_o \mathbf{Z}_c^H \mathbf{w} \tag{34}$$

and

$$P_k = < (\mathbf{w}^H \mathbf{Z}_c A_k \mathbf{V}_k^{oc}) (\mathbf{w}^H \mathbf{Z}_c A_k \mathbf{V}_k^{oc})^H >$$

$$= \tilde{V}_N^2 \mathbf{w}^H \mathbf{Z}_c \xi_k \mathbf{C}_k \mathbf{Z}_c^H \mathbf{w} \tag{35}$$

$$P_N = < (\mathbf{w}^H \mathbf{N}) (\mathbf{w}^H \mathbf{N})^H > = \tilde{V}_N^2 \mathbf{w}^H \mathbf{w} \tag{36}$$

Therefore,

$$\text{SINR} = \frac{\xi_o \mathbf{w}^H \mathbf{Z}_c \mathbf{C}_o \mathbf{Z}_c^H \mathbf{w}}{\mathbf{w}^H \mathbf{w} + \mathbf{w}^H \mathbf{Z}_c \Sigma \xi_k \mathbf{C}_k \mathbf{Z}_c^H \mathbf{w}} \tag{37}$$

## III. RESULTS, OBSERVATIONS AND DISCUSSIONS

This chapter discusses the results obtained and presents explanations of these observations. We first start by asking whether mutual coupling is at all significant and then proceed to look at how separation distance, noise level, scatterer radius and number of interference sources affect the performance of the array.

### A. SPATIAL CROSS CORRELATION

The first question we need to ask is whether the effect of mutual coupling is at all significant to an adaptive array? The importance of mutual coupling to diversity arrays has been addressed in [Ref. 7]. The parameter of interest is the spatial correlation of the field. It is an indication of the correlation of the voltage received between the elements of an array. One of the benefits of an array is to provide diversity; this means that while one element may be in the deep fade of the received signal pattern, hopefully another would still be in a position to receive the signal. For this to be true, the elements have to be relatively uncorrelated – hence a small value of spatial correlation means greater diversity.

Consider a two element array, distance d apart. In the absence of thermal noise, the voltage equations from (14) becomes :

$$V_1 = Z_{C\,11}\, V_1^{oc} + Z_{C\,12}\, V_2^{oc}$$

$$V_2 = Z_{C\,21}\, V_1^{oc} + Z_{C\,22}\, V_2^{oc}$$

Then the spatial cross correlation of the received electric field is defined as :

$$\rho = \langle V_1\, V_2^{*} \rangle = Z_{C\,11}\, Z_{C\,12}^{*} \langle V_1^{oc}\, V_1^{oc\,*} \rangle + Z_{C\,11}\, Z_{C\,22}^{*} \langle V_1^{oc}\, V_2^{oc\,*} \rangle + Z_{C\,12}\, Z_{C\,21}^{*} \langle V_2^{oc}\, V_1^{oc\,*} \rangle + Z_{C\,12}\, Z_{C\,22}^{*} \langle V_2^{oc}\, V_2^{oc\,*} \rangle \qquad (38)$$

$$\langle V_1^{oc} V_1^{oc\,*} \rangle = \langle V_2^{oc} V_2^{oc\,*} \rangle = 1 \tag{39}$$

and $$\langle V_1^{oc} V_2^{oc\,*} \rangle = \langle V_2^{oc} V_1^{oc\,*} \rangle = J_o (k_o d) \quad \text{[Ref. 4]} \tag{40}$$

where $$Z_{C11} = Z_{C22} \ , \ Z_{C12} = Z_{C21} \tag{41}$$

$J_o$ (.) = Bessel's function of first kind, order zero.

Thus

$$\rho = (Z_{C11} Z_{C12}^{*} + Z_{C12} Z_{C11}^{*}) + (Z_{C11} Z_{C11}^{*} + Z_{C12} Z_{C12}^{*}) J_o(k_o d) \tag{42}$$

Extracting the common factor and substituting for $\mathbf{Z}_C$, the spatial cross correlation of the electric field for a two element array terminated in $Z_L = Z_{11}^{*}$ is given by [Ref. 4] :

$$\rho = \rho_{oc} - \frac{R_{12}}{R_{11}\left(1 + \frac{|Z_{12}|^2}{4R_{11}^2}\right)} \tag{43}$$

where $\rho_{oc} = J_o(k_o d)$ is the correlation in the absence of mutual coupling, and $R_{11}$ and $R_{12}$ are the real parts of $Z_{11}$ and $Z_{12}$ respectively. Fig 3.1 below shows the spatial cross correlation vs separation distance d between two half-wavelength dipoles.

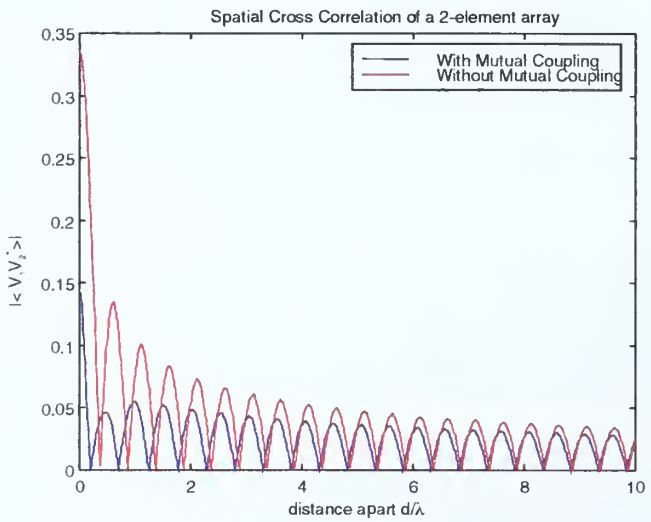


Fig 3.1 Spatial Cross Correlation of a 2 element array

As expected, at longer separation, the effect of mutual coupling is diminished and the two curves converge. However, there is a marked difference for $d<\lambda$, which indicates the significance of including mutual coupling.

Another way to interpret spatial cross correlation is to examine the normalized spatial cross correlation (Fig 3.2). For reference, we have indicated the correlation values of 0.7 and 0.3 (Table 3.1). It is seen that for this example the effect of mutual coupling is to decorrelate the signals initially but correlate them more for larger values of spacing d.

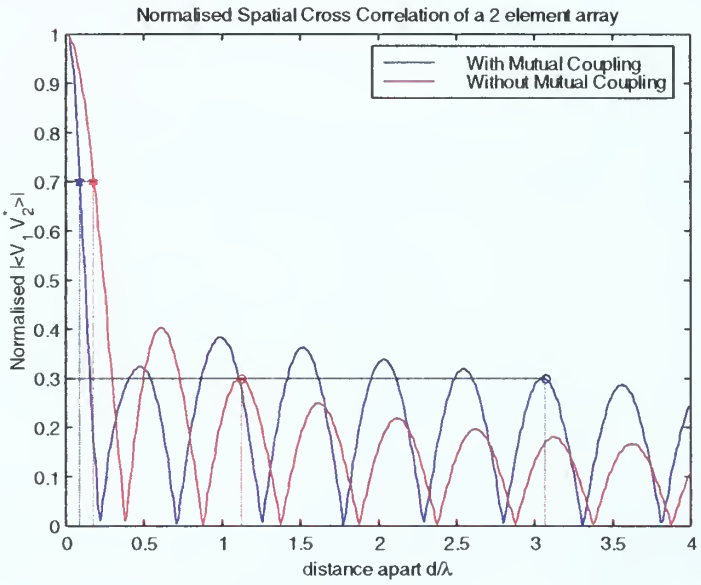


Fig 3.2 Normalized Spatial Cross Correlation Electric Field in a 2 element array

| | Values of d/λ | |
|---|---|---|
| | Without mutual coupling | With mutual coupling |
| $\rho \leq 0.3$ | $\geq 1.1201$ | $\geq 3.0701$ |
| $\rho \leq 0.7$ | $\geq 0.1801$ | $\geq 0.0901$ |

Table 3.1 Values of spacing d for $\rho \leq 0.3$ and 0.7

While both curves fall rapidly below the upper level of 0.7, there is a large difference in the lower level of 0.3; without mutual impedance, the arrays have minimal spatial cross correlation (<0.3) for $d>1.12\lambda$, whereas with mutual coupling, this occurs only after $d>3.07\lambda$. What this means is that in the presence of mutual coupling, the array diversity will be generally reduced.

## B. EFFECT OF MUTUAL COUPLING ON WEIGHTING VECTOR

Another effect of mutual coupling is in the resultant weights. Using (18), we observe that we get different weighting functions when considering and ignoring the effects of mutual impedance (Table 3.2). The weights are normalized such that $w^H w = 1$.

| | | |
|---|---|---|
| Number of elements | $N = 4$ | |
| Separation between elements | $d = \lambda/4$ | |
| Number of interference sources | $K = 3$ | |
| Direction of desired source | $\overline{\phi}_o = 90°$ | |
| Directions of interference sources | $\overline{\phi}_k = 30°, 60°, 120°$ | |
| Scatter radii | $r_o = r_k = 0$ | |
| Consider mutual coupling w (normalized) | Ignore mutual coupling $w_o$(normalized) | Deterministic case $w_d$(normalized) |
| 0.2624-0.1203i | 0.3911+0.0261i | 0.3300 |
| -0.4627-0.2327i | -0.3631-0.4631i | -0.5357-0.3227i |
| 0.4330+0.5600i | 0.2335+0.5445i | 0.4275+0.4564i |
| 0.2102-0.3211i | 0.1704-0.3530i | -0.0689-0.3227i |

Table 3.2 Weights for adaptive MMSE and deterministic cases

Table 3.2 also shows the weights $w_d$ calculated in the deterministic case, that is, where it is assumed that the directions of the interference sources are known and the weights calculated such that nulls are steered in the directions of the interferences. Since

the weighting vectors are all different, we would expect different beam patterns using these 3 solutions, as shown in Fig 3.3 below. Values of the corresponding SINR are indicated in the inset.

Note : In Fig 3.3 and subsequent plots, the blue curve corresponds to adaptive (MMSE) solution using eqn (18) , with mutual coupling considered. This means that the off diagonal terms of Z are non-zero and are given by (6). The red curve corresponds to adaptive solution also given by (18), this time ignoring mutual coupling (Z in (13) is diagonal). The green curve corresponds to the solution in the deterministic case, calculated without mutual coupling. Moreover, the direction of the desired source is maintained at $\bar{\phi}_o$=90° (unless otherwise specified) and is denoted by a blank circle on the abcissa. Pink asterisks (*) denote the directions of the interference sources.

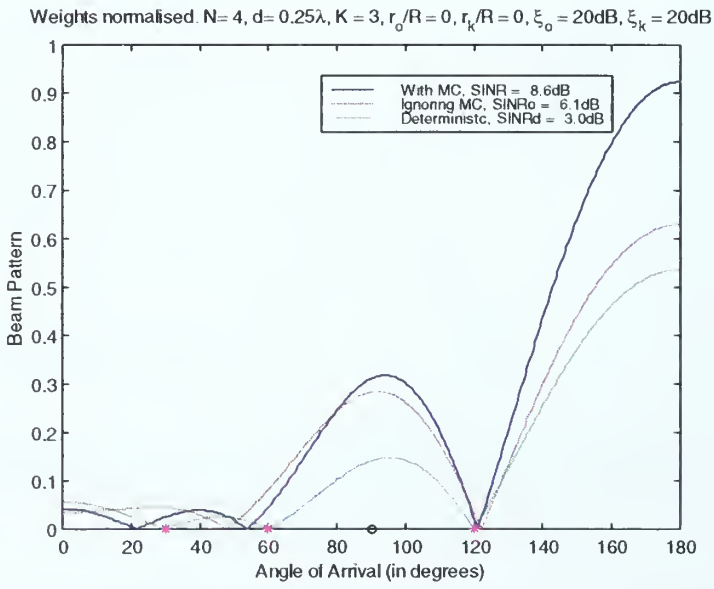


Fig 3.3 Beam pattern for adaptive solutions considering and ignoring mutual impedance and deterministic weights.
All weights normalized such that $w^H w=1$, beam pattern not normalized.

In Fig 3.3, it is seen that although nulls are steered in the directions of the interference sources in the deterministic case (green), it does not provide the best SINR. This is because in the other cases (adaptive solutions – blue and red), the gain in the direction of the desired signal is higher than the deterministic case (which does not take into account direction of desired signal), thereby contributing to a higher desired signal power received, $P_o$ in (34). This thus gives rise to higher SINR.

Fig 3.3 shows the beam pattern (un-normalized) using weights calculated. However, it is often the normalized beam pattern that is more suitable for comparison between the three solutions; in Fig 3.4 and subsequent graphs, the beam patterns are normalized to the maximum gain.

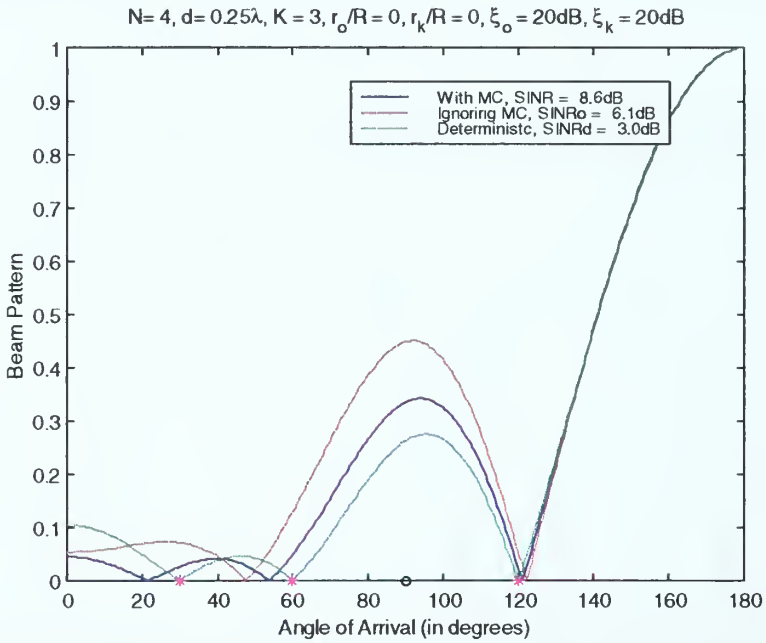


Fig 3.4 Beam pattern (normalized to max gain) for adaptive solutions considering and ignoring mutual impedance and using deterministic weights

Fig 3.3 and Fig 3.4 are essentially the same beam patterns, though in Fig 3.4 the adaptive, no-mutual-coupling solution (red) seems to have a higher gain in the direction of the desired source ($\bar{\phi}_o = 90°$) than the mutual coupling case (blue). As such, one might be

lulled into expecting the red curve to have a higher SINR; it should be borne in mind that the graph shows relative gains only. For a true value of the SINR values, one should always refer to the values displayed in the inset rather than to the heights of the curves.

The previous two sections show that mutual coupling does have an effect on the performance of adaptive array antennas. This effect obviously diminishes as the physical separation between the elements increases.

## C. EFFECT OF ELEMENT SEPARATION

An interesting comparison would be how the SINR is affected by varying the separation distance d between elements. Fig 3.5 below shows the SINR vs d plot for a 4-element array antenna in a 3 interference situation (no scatterers).

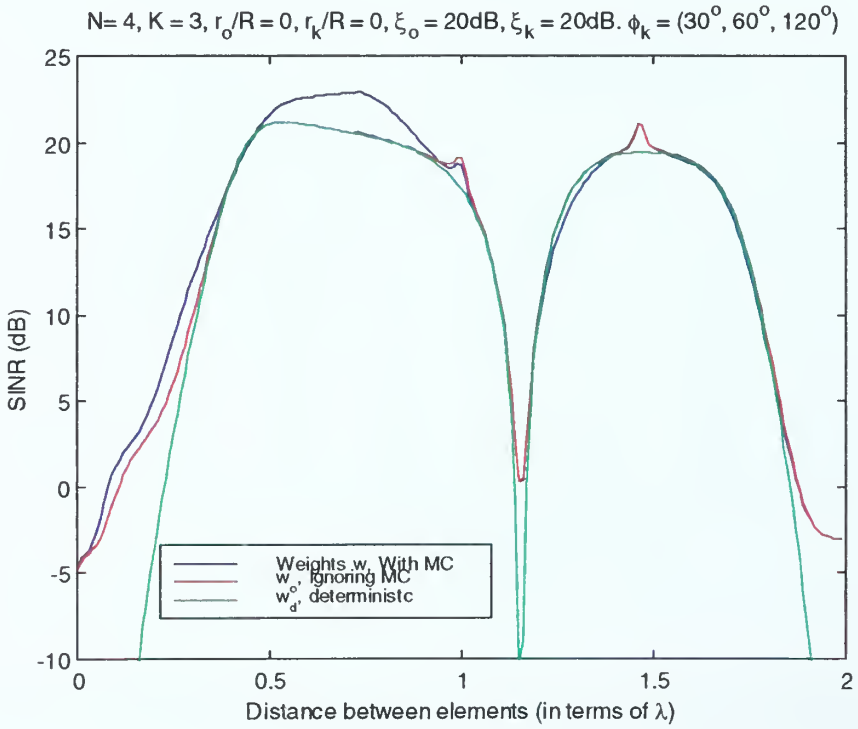


Fig 3.5 SINR vs d

It is seen that the SINRs with and without mutual coupling do show differences for small values of d (less than 1λ), sometimes by as much as 3dB (e.g. at d≈0.75λ). At higher separations, they are about the same, as expected since mutual coupling effect is diminished. In all cases, the SINR using the adaptive solution (no mutual coupling) is consistently higher than that using the deterministic weights. At the same time, there are differences between the adaptive solutions with and without mutual coupling (blue and red curves in Fig 3.5). The exact difference is difficult to quantify as it is case specific: in Fig 3.5 above, the situation is for a 4 element array in a 3 interference environment ($\bar{\phi}_k$ = 30°, 60° and 120°) with $\xi_o = \xi_k$ = 20dB.

An interesting feature is the fact that the SINR drops drastically near d=1.15λ. This is shown in Fig 3.6 below.

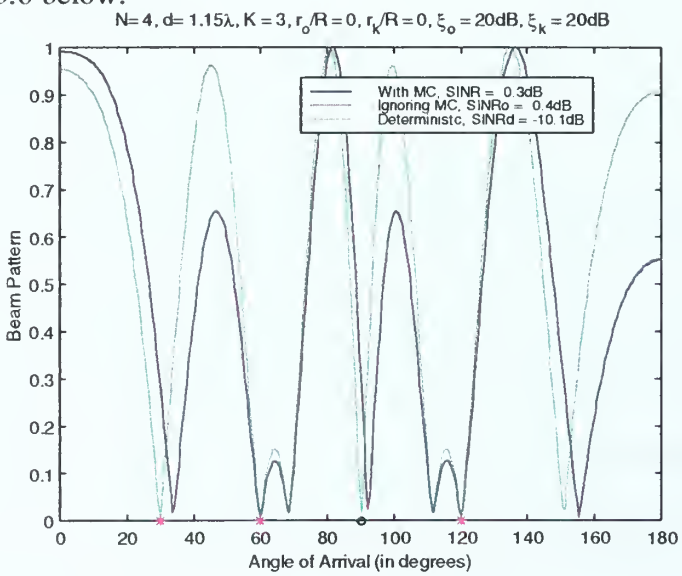


Fig 3.6 Beam pattern for d = 1.15λ

A closer examination reveals that this drop is due to the rather low angular response of the array in the direction of the main source. Therefore, in practical design of array antennas, it would be wise not to exceed d=λ/2 unless we impose an additional

constraint that the pattern not go to zero in the direction of the desired source. In this paper, we shall continue to study the cases for d up to $1\lambda$.

## D. EFFECT OF NOISE

From (18) and (14), we have :

$$\mathbf{w_{opt}} = \Phi^{-1}\,\mathbf{S}$$

$$= [\,\mathbf{U} + \mathbf{Z_c}\,\xi_o\,\mathbf{C_o}\,\mathbf{Z_c}^{H} + \mathbf{Z_c}\,\Sigma\,\xi_k\,\mathbf{C_k}\,\mathbf{Z_c}^{H}\,]^{-1}\,\mathbf{Z_c}\,\mathbf{C_s}$$

and $$\mathbf{V_t} = \mathbf{Z_c}\,\mathbf{V^{oc}} + \mathbf{N}(t)$$

In the situation where $\xi_o >> 1$, $\xi_k >> 1$, we get $|\mathbf{V^{oc}}| >> |\mathbf{N(t)}|$ so

$$\mathbf{w_{opt}} \approx [\,\mathbf{Z_c}\,(\xi_o\,\mathbf{C_o})\,\mathbf{Z_c}^{H} + \mathbf{Z_c}\,(\Sigma\,\xi_k\,\mathbf{C_k})\,\mathbf{Z_c}^{H}\,]^{-1}\,\mathbf{Z_c}\,\mathbf{C_s} \qquad (44)$$

and $$\mathbf{V_t} \approx \mathbf{Z_c}\,\mathbf{V^{oc}} \qquad (45)$$

The resultant signal is

$$S_r = \mathbf{w_{opt}}^{H}\,\mathbf{V_t}$$

$$\approx \{[\,\mathbf{Z_c}\,\xi_o\,\mathbf{C_o}\,\mathbf{Z_c}^{H} + \mathbf{Z_c}\,\Sigma\,\xi_k\,\mathbf{C_k}\,\mathbf{Z_c}^{H}\,]^{-1}\,\mathbf{Z_c}\,\mathbf{C_s}\}^{H}\,\mathbf{Z_c}\,\mathbf{V^{oc}}$$

$$= \mathbf{C_s}^{H}\,\mathbf{Z_c}^{H}\,\{[\,\mathbf{Z_c}\,\xi_o\,\mathbf{C_o} + \Sigma\,\xi_k\,\mathbf{C_k}\,\mathbf{Z_c}^{H}\,]^{-1}\}^{H}\,\mathbf{Z_c}\,\mathbf{V^{oc}}$$

$$= \mathbf{C_s}^{H}\,\mathbf{Z_c}^{H}\,\{(\mathbf{Z_c}^{H})^{-1}\,(\xi_o\,\mathbf{C_o} + \Sigma\,\xi_k\,\mathbf{C_k})^{-1}\,\mathbf{Z_c}^{-1}\}^{H}\,\mathbf{Z_c}\,\mathbf{V^{oc}}$$

$$= \mathbf{C_s}^{H}\,\mathbf{Z_c}^{H}\,(\mathbf{Z_c}^{-1})^{H}\,[(\xi_o\,\mathbf{C_o} + \Sigma\,\xi_k\,\mathbf{C_k})^{-1}]^{H}\,[(\mathbf{Z_c}^{H})^{-1}]^{H}\,\mathbf{Z_c}\,\mathbf{V^{oc}}$$

$$= \mathbf{C_s}^{H}\,(\mathbf{Z_c}^{-1}\mathbf{Z_c})^{H}\,[(\xi_o\,\mathbf{C_o} + \Sigma\,\xi_k\,\mathbf{C_k})^{-1}]^{H}\,[\mathbf{Z_c}^{H}\,(\mathbf{Z_c}^{H})^{-1}]^{H}\,\mathbf{V^{oc}}$$

$$= \mathbf{C_s}^{H}\,[(\xi_o\,\mathbf{C_o} + \Sigma\,\xi_k\,\mathbf{C_k})^{-1}]^{H}\,\mathbf{V^{oc}} \qquad (46)$$

which turns out to be independent of $\mathbf{Z}_c$. Since the effect of mutual interference is in the impedance matrix $\mathbf{Z}_c$, it is predicted that when $\xi_o$ , $\xi_k$ is large ($\geq$40dB), the effect of mutual impedance is reduced and the two adaptive solutions (blue and red in Fig 3.7) converge. (Recall that $\xi_o$ = input signal (desired source) to thermal noise ratio and $\xi_k$ = input interference ($k^{th}$ interfering source) to thermal noise ratio )

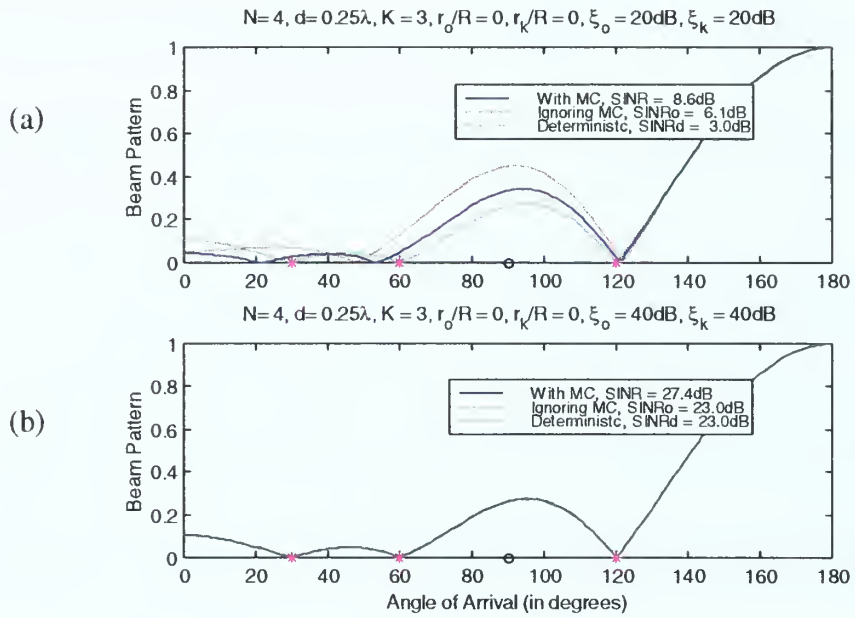


Fig 3.7 Comparison of the effect of noise

Fig 3.7a shows the beam patterns using the different weights when $\xi_o = \xi_k = 20$dB. However, when signal-to-noise-ratio $\xi_o$ and interference-to-noise-ratio $\xi_k$ are increased (to 40dB) as in Fig 3.7b, one can easily observe that the solutions (with and without mutual coupling) converge, as predicted. It is important to note that though the normalized beam patterns in Fig 3.7b are similar, the weights and terminal voltages with and without mutual coupling are not the same. This is evident in the fact that the SINR values with and without mutual coupling differ by as much as 4dB in Fig 3.7b. This is because the noise levels in the three cases are different relative to the output signal.

## E. EFFECT OF SCATTERER RADII $r_o$ , $r_k$

Recall that in our model outlined in Section 2A that the desired and interference sources are at distance $R_k$ from the array. In addition, each source is embedded in a scattering environment, in which the scatterers are assumed to be distributed uniformly around each source over a circular region of radius $r_k$ (k=0,1,....K). Here we take $R_k$ = 1 km and vary the values of $r_k$ (k=0,1,....K); ultimately, it is the ratio $b_k = \frac{r_k}{R}$ that is significant in the calculations.

It was found that the effect of the scatterer radii $r_o$ and $r_k$ depend on the input signal to noise ratios $\xi_o$ and $\xi_k$ . First we compare the effect of increasing scatterer radius $r_o$ while maintaining $r_k$ = 0. For illustration, a 4-element array with λ/2 spacing is used in a 3 interference situation ($\bar{\phi}_k$ = 30°, 45°, 60°). Fig 3.8 below shows the resultant normalized beam pattern.

(a)

(b)

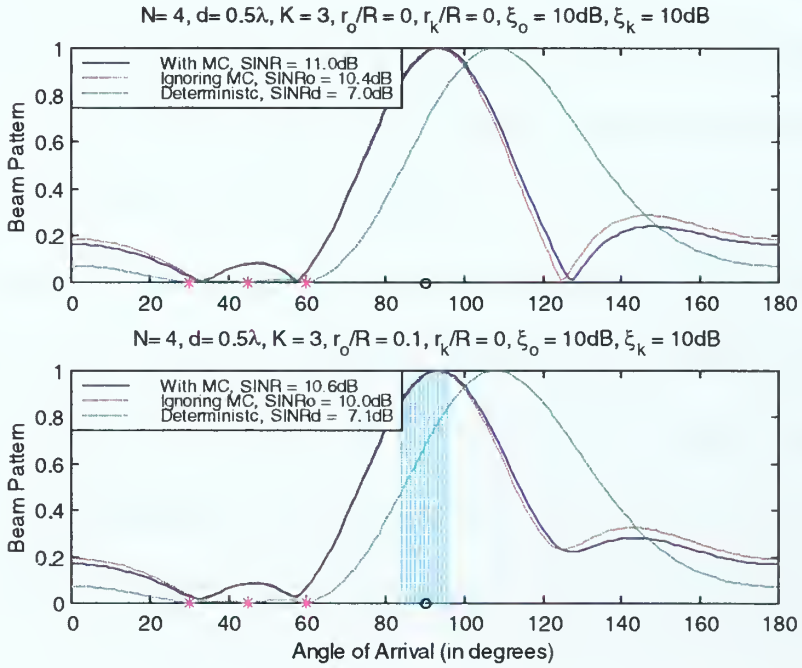

In Fig 3.8a, there are no scatterers around the desired source ($r_o = 0$) whereas in Fig3.8b, scatterers are present ($r_o/R = 0.1$). We can see that the weights and (hence) beam patterns are changed slightly, and that with scatterers (Fig 3.8b) the resultant SINR values are slightly reduced. The light blue column shows the extent of the angular spread of the desired signals; hence the area in the column under each curve would represent the amount of power arriving from the source. In the calculation of SINR, this area is divided by the angular spread to give an average value of the signal. Whether this average value is greater or smaller than the SINR in the no-scatterer case obviously depends on the shape of the curve. In Fig 3.8 above, it is observed that though the average SINR values for adaptive solutions are smaller, the deterministic solution actually shows an improvement in the averaged case.

Nonetheless, it is important to note that the adaptive solutions (blue and red) still give greater SINR than the deterministic case (green). This is in accordance with our conjecture that the adaptive MMSE solution also leads to the Maximum SINR solution. It has been shown in [Ref. 4] that the SINR without mutual coupling and no scatterers around the desired source is always better than the deterministic case. No such conclusion can be drawn when mutual coupling is taken into account.

Next we investigate the situation when $\xi_o$ and $\xi_k$ are increased to 20dB (Fig 3.9); comparing the 4 cases (in Fig 3.8 and Fig 3.9), the deterministic case remains the same since the deterministic weights do not depend on $r_o$ , $r_k$ , $\xi_o$ nor $\xi_k$. The adaptive solutions change accordingly - most surprising is the fact that for $r_o/R = 0.1$, $r_k/R = 0$, $\xi_o = \xi_k =$ 20dB (Fig 3.9b), the adaptive solutions (both with and without mutual coupling) give

SINR values smaller than the deterministic case. This is in contrast to the no-scatterer case where the adaptive (MMSE) solutions always give the maximum SINR.

(a)

(b)

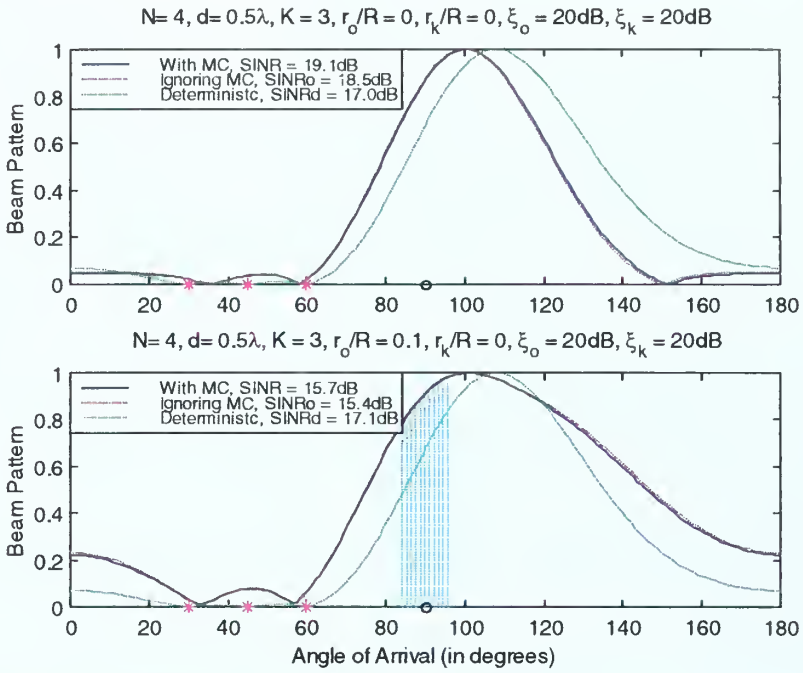


Fig 3.9 Effect of scatterer radius $r_o$ ($\xi_o$ and $\xi_k$ = 20dB)

Next we examine the effect of increasing the scatterer radius $r_k$ while maintaining $r_o$ =0. In Fig 3.10 below, the columns in magenta represent the angular spread of the interference signal from the interference sources. The increment of $r_k$ again reduces the SINR but not as much as in the case of scatterers around the desired source. The decrease in SINR is expected since scatterers increase the directions from which the interference signals can now reach the array, thereby increasing the interference power received. In this case the increment of $r_k$ does not change the fact that adaptive solutions still give greater SINR than the deterministic case.

(a)

(b)

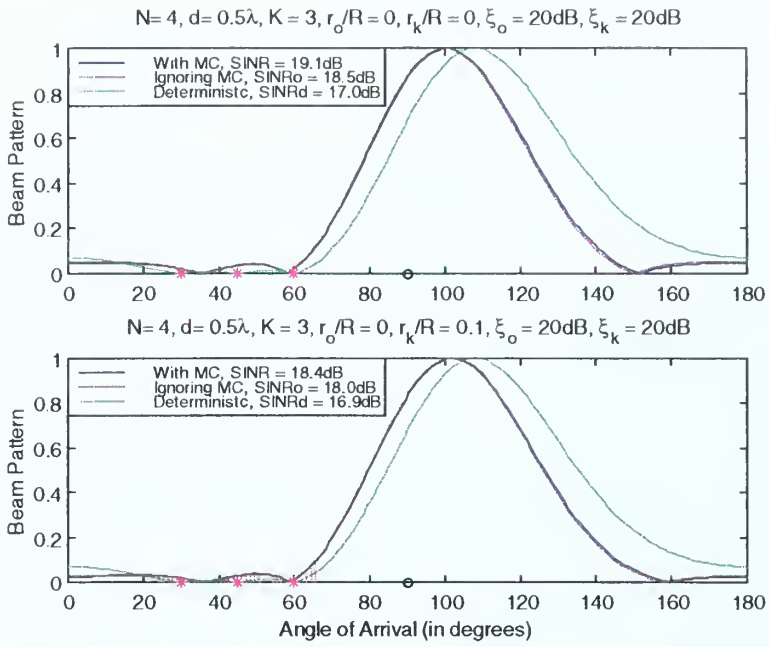


Fig 3.10 Effect of scatterer radius $r_k$ ($\xi_o$ and $\xi_k$ = 20dB)

## F. EFFECT OF NUMBER OF INTERFERENCE SOURCES K

Another variable parameter is K, the number of interference sources. In Fig 3.11 below, a 4-element array (N=4) is placed in an environment where there are no scatterers around any of the sources ($r_o = r_k = 0$).

(a)

(b)

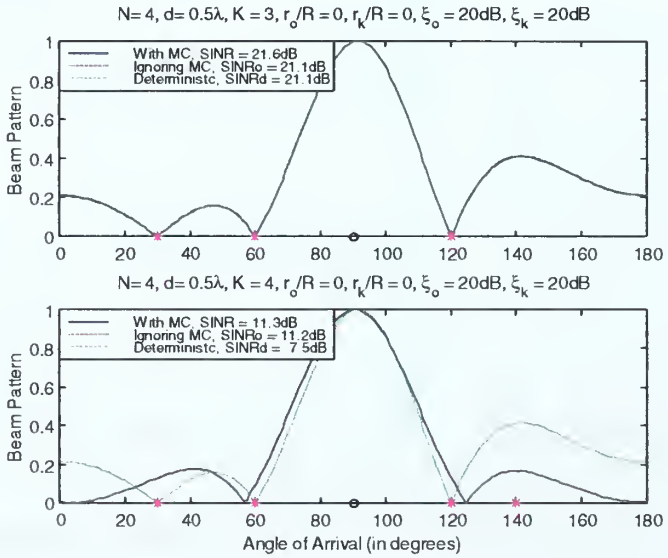


Fig 3.11 Effect of Number of Interference Sources K (K>N-1)

In Fig 3.11a, 3 interference sources (K=3) have been specified in the directions $\bar{\phi}_k = 30^o, 60^o, 120^o$. The adaptive solutions and the deterministic solution are similar and all steer nulls in the directions $30^o$, $60^o$, $120^o$ that effectively cancel out the interference sources. The resultant SINRs for all 3 cases are therefore very close. In Fig 3.11b, an additional interference source has been added (at $\bar{\phi}_k = 140^o$). With the deterministic weights, a maximum of N-1 nulls can be chosen; this means we can (arbitrarily) choose only 3 of the 4 interference sources to cancel. With the adaptive solutions specified by (18), the weights are altered to give a different beam pattern as shown. Though none of the nulls is exactly in the direction of the interference sources, the 'spreading' of the pattern is such that the resultant SINR is greater than that given by the deterministic case.

In Fig3.12 below, the same situations are compared, this time with scatterers around all sources.

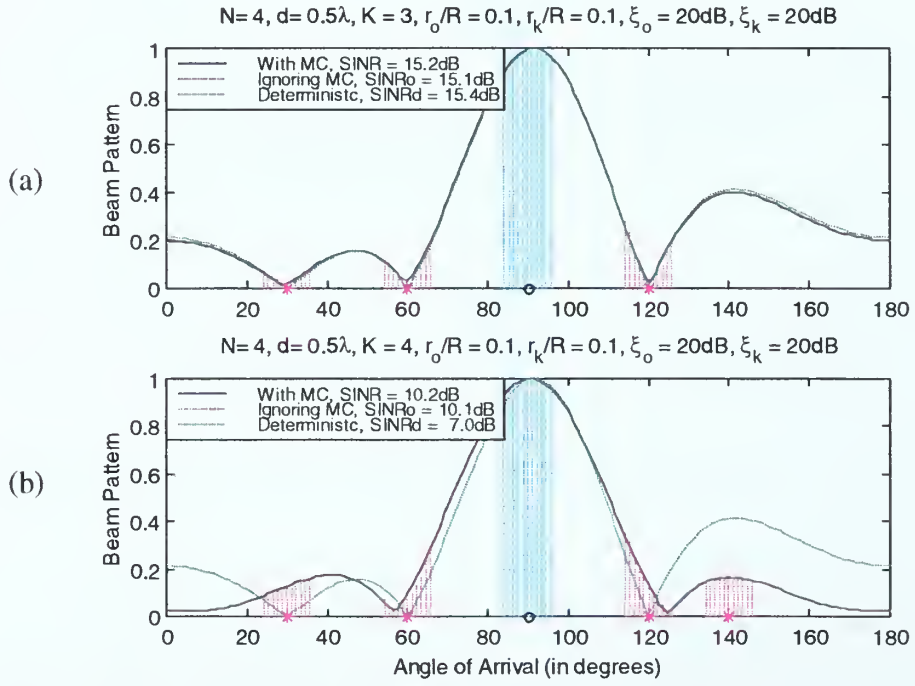


Fig 3.12 Effect of Number of Interference Sources K (K>N-1)

In Fig3.12a, we note that the deterministic SINR is better than for the adaptive cases (as discussed previously in Section E). However, with the addition of a fourth interferer at $\bar{\phi}_k = 140^o$, the adaptive cases actually perform better than the deterministic solution in terms of SINR. This emphasizes the flexibility of the adaptive solution in encountering more than N-1 inteference sources.

At the other extreme, we would like to examine the situations where the number of inteferers K is less than the number of array elements N. To illustrate, we consider N=6 and 8 in an environment with only 3 interference sources. Fig 3.13 below shows the resultant normalized beam patterns.

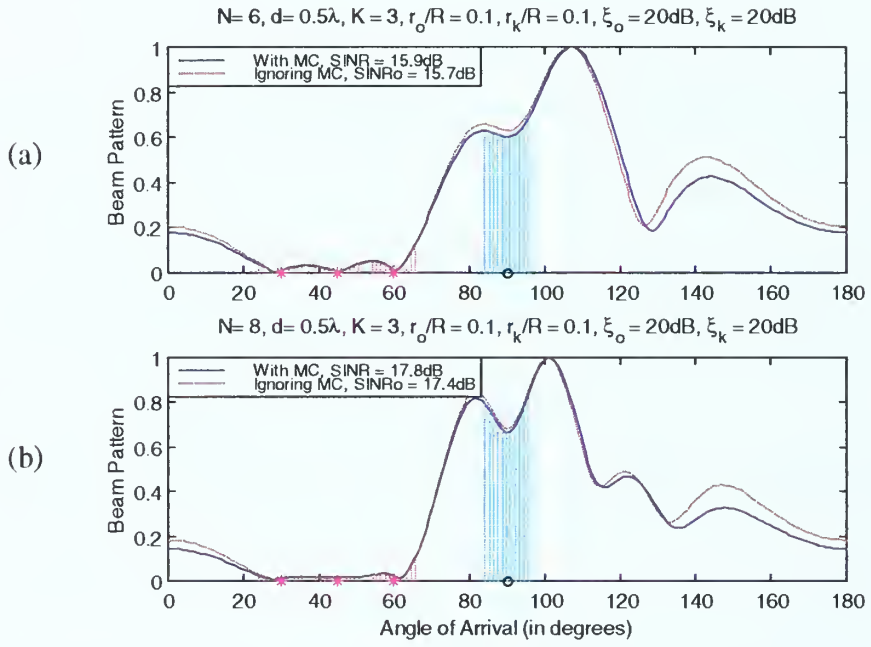


Fig 3.13 Effect of Number of Interference Sources K (K<N-1)

It is seen that when K < N-1 ("there are more than enough array elements to go around"), the SINR using the adaptive solutions are improved. Table 3.3 below shows these values for N=4,6,8,10 and 30 (K=3 in all cases).

| | K = 3 d = λ/2 $\frac{r_o}{R}=\frac{r_k}{R}=0.1$ $\xi_o = \xi_\kappa = 20$dB | | | | |
|---|---|---|---|---|---|
| | N=4 | N=6 | N=8 | N=10 | N=30 |
| SINR (with mutual coupling) | 15.4dB | 15.9dB | 17.8dB | 18.2dB | 18.5dB |
| SINR (ignore mutual coupling) | 15.2dB | 15.7dB | 17.4dB | 17.7dB | 18.0dB |
| SINR (deterministic case based on N=4) | 16.9dB | 16.9dB | 16.9dB | 16.9dB | 16.9dB |

Table 3.3 Comparison of SINR

As is obvious from the table, as the number of array elements (N) increases, the SINR increases as well for the adaptive cases. Of course, the deterministic case does not change since it is dependent only on the direction of the interferers. Initially, we note that SINR (deterministic) is greater than SINR(adaptive) – this was discussed in Section 3E as being due to scatterers around the desired source. However, for higher values of N (N≥ 8 in this example), we find that the SINR of the adaptive solutions actually increases to greater than that offered by the deterministic case. Beyond a certain value of N, this increment becomes insignificant or non-efficient (c.f. SINR for N=10 and 30). Nonetheless, this is another indication of the ability of the adaptive algorithm in making full use of its elements to find the best solution.

## G. ANGULAR RESOLUTION OF SOURCES

Our next area of interest is in examining if the use of an adaptive array is effective when the various sources are closely spaced. Consider the situation where one of the interferers is very close to the desired source : $\bar{\phi}_o$ = 90°, $\bar{\phi}_k$ = 90°-2.85° = 87.15° (2.85°

was chosen as it is the rms value of angular spread for $\frac{r_o}{R} = \frac{r_k}{R} = 0.1$ as in eqn (5) ). This is shown in Fig 3.14.

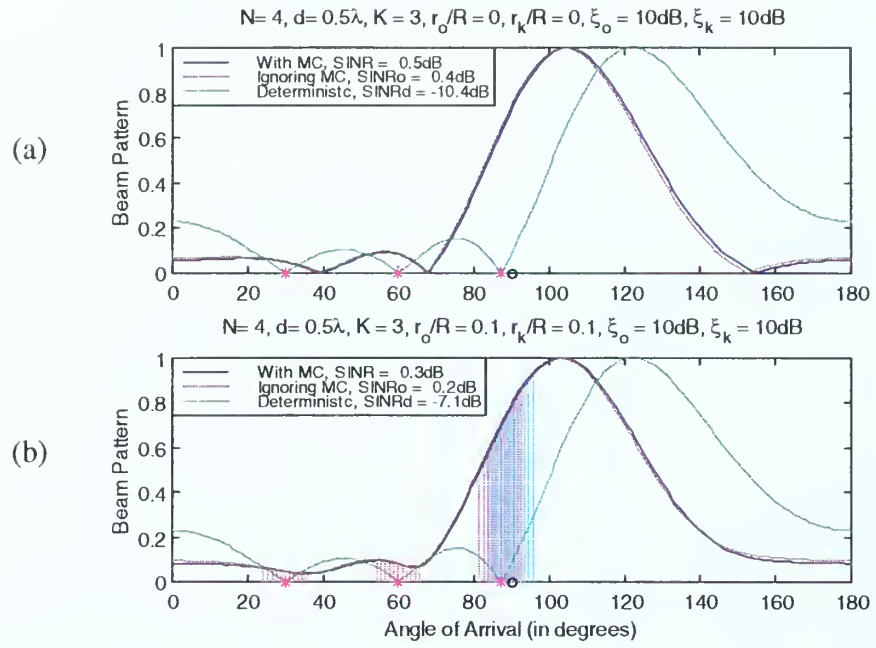


3.14 Effect of Interference Source close to Desired Source ($\xi_o$ and $\xi_k$ = 10dB)

Fig 3.14a shows the situation where there are no scatterers around any of the sources. It is seen that the close proximity of a null near the desired source lowers the SINR in the deterministic case drastically, whereas for the adaptive solutions, the nulls are actually steered away so as to give a significantly better SINR. In Fig 3.14b, the presence of scatterers does affect the performance of the adaptive solutions, but it is seen that the adaptive solutions still give better SINR values.

Fig3.15a and b below shows the same situations with $\xi_o$ and $\xi_k$ increased to 40dB. As discussed in Section D, high values of $\xi_o$ and $\xi_k$ mean that the solutions all converge to the deterministic case. However, in the presence of interference close to the desired source, the solutions are different. More significantly, the SINR from the adaptive

solutions in this case is lower than that from the deterministic case – again, this is due to the presence of scatterers around the desired source.

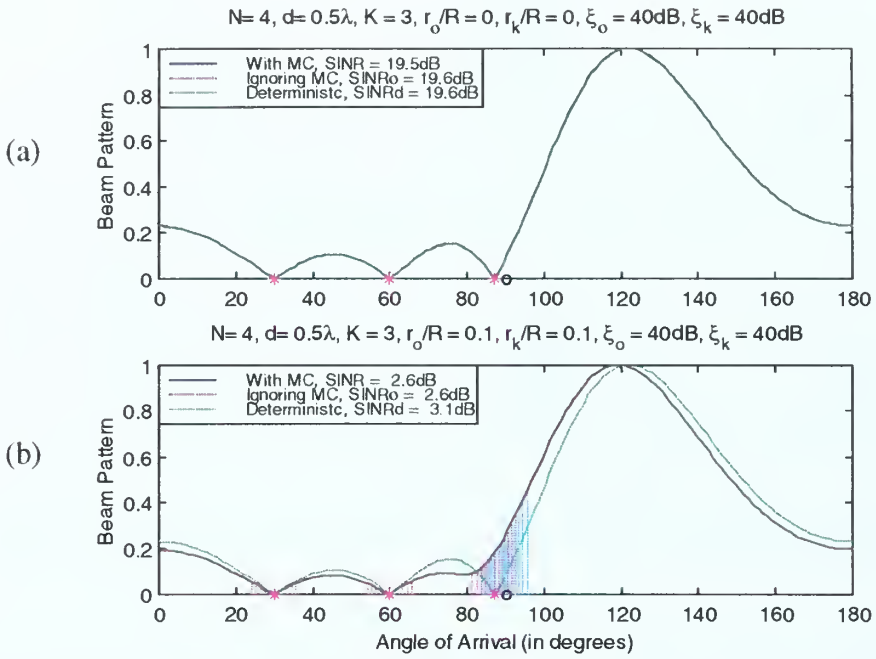


3.15 Effect of Interference Source close to Desired Source ($\xi_o$ and $\xi_k$ = 40dB)

What happens when an interference source, initially remote from the desired source, is moved close to it? In Fig 3.16a below, $\bar{\phi}_k$ = 30°, 45° and 60° while in Fig 3.16b, the interference source at $\bar{\phi}_k$ = 45° is moved to 87.15°.

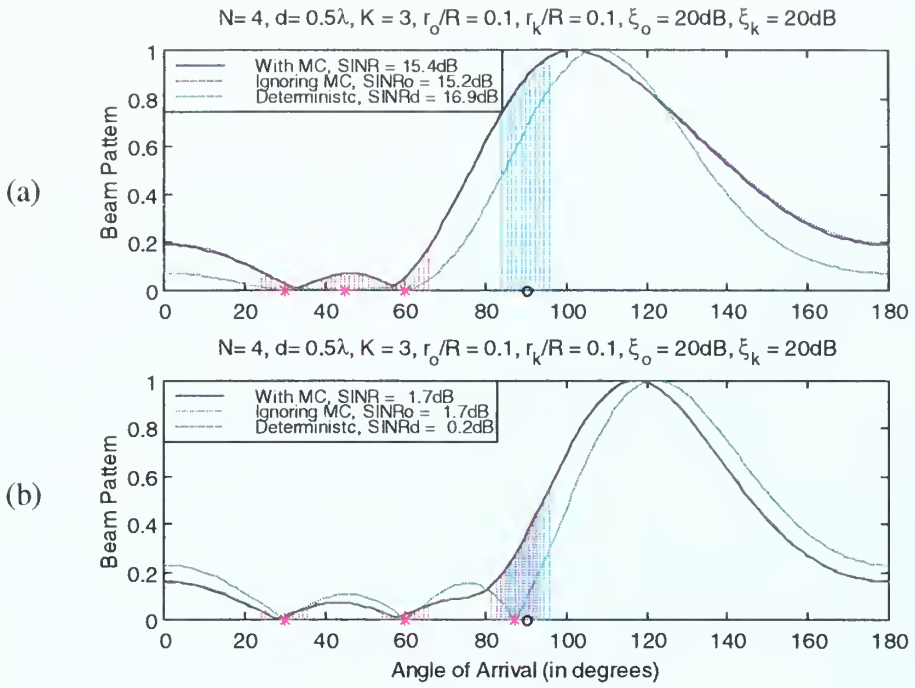


Fig 3.16 Effect of Interference Source close to Desired Source ($\xi_o$ and $\xi_k$ = 20dB)

In a previous section, it was shown that when there are scatterers around the desired source, the deterministic solution gives a greater SINR than the adaptive solution, as shown in Fig 3.16a. However, this is reversed when one of the interference sources is moved close to the desired (Fig 3.16b). This shows that when an interference source is close to the desired source, the adaptive solution performs better than the deterministic one, even when there are scatterers around the desired source.

# IV SUMMARY AND CONCLUSIONS

## A. SUMMARY

Through the series of results obtained, the effect of mutual coupling on the performance of adaptive array antennas was studied by varying several parameters. These can be summarized as follows:

### 1. Effect of Mutual Coupling on Spatial Cross Correlation

The effect of mutual coupling is to reduce the spatial cross correlation initially (for $d < 1\lambda$) but to increase it for larger values of inter-element spacing d.

### 2. Effect of Separation Distance d

For $d>1\lambda$, there is practically no difference on the SINR obtained with and without considering mutual coupling. At lesser separation, however, the difference is significant and can be as much as 3dB.

### 3. Effect of Noise

When the signal-to-noise-ratios $\xi_o$ and $\xi_k$ are high (>40dB), it was found that the solutions obtained with and without considering mutual coupling are very close, and converge to the deterministic solution (provided number of interference K < number of array elements N).

### 4. Effect of Scatterer Radii $r_o$ and $r_k$

When the scatterer radii $r_o$ and $r_k$ are increased, in general, the SINR of the solutions are reduced, This is expected as it represents uncertainty in the directions of arrival of the sources.

When the scatterer radius $r_o$ is increased, at a critical $\xi_o$, $\xi_k$ level, the adaptive MMSE solutions cease to give Maximum SINR. This is in contradiction to the conjecture that MMSE and Maximum SINR solutions are equivalent [Ref. 6: p41].

On the other hand, increasing the scatterer radius $r_k$ alone does not 'invert' this trend of MMSE solution giving max SINR.

### 5. Effect of Number of Interference Sources K

When the number of interferers K ≥ the number of array elements N, the deterministic solution can do no better than pointing N-1 nulls towards the interferers. The adaptive solutions, however, seeks to minimize the error and generally gives a greater SINR than the deterministic case.

When the number of interferers K < the number of array elements N, it was found that the adaptive algorithm makes use of this fact to improve the SINR. Hence even with scatterers around the desired source (as in the previous section), with a sufficient number of array elements, the adaptive solution will give an SINR greater than that in the deterministic case.

### 6. Angular Resolution of Sources

In cases where one of the interferers is very close to the desired source, it was found that adaptive solutions perform better than deterministic one. This includes the situation where there are scatterers around the desired source and demonstrates the excellent angular resolution offered by adaptive arrays.

## B. CONCLUSIONS

We have examined the effect of mutual coupling on the performance of an adaptive array in a realistic communications environment, where the desired and interference sources are embedded in an area of scattering objects. Expressions for the MMSE solutions and SINR were derived for this scenario. These were subsequently used to show the effect of mutual coupling, in particular in array where the element separation was less than $1\lambda$. The effects of the other parameters in the system were also discussed, including conditions under which the MMSE solution does not give rise to Maximum SINR.

# APPENDIX A : EXPRESSIONS FOR Φ AND S

## A. EXPRESSION FOR Φ

From (15),

covariance matrix $\Phi = \langle \mathbf{V_t}\, \mathbf{V_t}^{H} \rangle$

$$= \langle (\mathbf{Z_c}\, \mathbf{V}^{oc} + \mathbf{N})\, (\mathbf{Z_c}\, \mathbf{V}^{oc} + \mathbf{N})^{H} \rangle$$

$$= \mathbf{Z_c} \langle \mathbf{V}^{oc}\, \mathbf{V}^{oc\,H} \rangle \mathbf{Z_c}^{H} + \mathbf{Z_c} \langle \mathbf{V}^{oc}\, \mathbf{N}^{H} \rangle \qquad \text{(A1)}$$

$$+ \langle \mathbf{N}\, \mathbf{V}^{oc\,H} \rangle \mathbf{Z_c}^{H} + \langle \mathbf{N}\, \mathbf{N}^{H} \rangle$$

Now, consider the terms separately :

(i) Second and third terms :

Assuming noise is zero mean and uncorrelated with signal,

then $\langle a_o\, e^{-j(\omega_o t + \beta_o)}\, \mathbf{N}(t) \rangle \propto \langle \mathbf{N}(t) \rangle = 0$

(A2)

so $\langle \mathbf{V_t}^{oc}\, \mathbf{N}^{H} \rangle = \langle \mathbf{V_t}^{oc} \rangle \langle \mathbf{N}^{H} \rangle = 0 = \langle \mathbf{N}\, \mathbf{V_t}^{oc\,H} \rangle$ (A3)

(ii) Fourth term :

Assuming noises at the ports are uncorrelated with each other

$$\langle \mathbf{N}\, \mathbf{N}^{H} \rangle_{mn} = \delta_{mn}\, \tilde{V}_N^2$$

(A4)

where $\tilde{V}_N$ = root mean square noise voltage

(iii) First term :

$$\langle \mathbf{V_t}^{oc}\, \mathbf{V_t}^{oc\,H} \rangle = \langle [a_o\, e^{j(\omega t + \beta o)}\, \mathbf{V_o}^{oc} + \Sigma\, a_k\, e^{j(\omega t + \beta k)}\, \mathbf{V_k}^{oc}\,]$$

$$\cdot\, [a_o\, e^{-j(\omega t + \beta o)}\, \mathbf{V_o}^{oc\,H} + \Sigma\, a_l\, e^{-j(\omega t + \beta l)}\, \mathbf{V_l}^{oc\,H}\,] \rangle$$

$$= \langle a_o^{\,2}\, \mathbf{V_o}^{oc}\, (\mathbf{V_o}^{oc})^{H} \rangle + \Sigma \langle a_o\, a_k\, e^{j(\beta k - \beta o)}\, \mathbf{V_k}^{oc}\, (\mathbf{V_o}^{oc})^{H} \rangle \qquad \text{(A5)}$$

$$+\Sigma < a_o a_k e^{j(\beta o - \beta k)} \mathbf{V}_o^{oc} (\mathbf{V}_k^{oc})^H > +\Sigma\Sigma < a_k a_l e^{j(\beta k - \beta l)} \mathbf{V}_k^{oc} (\mathbf{V}_l^{oc})^H >$$

$$\text{Now } < a_o^2 \mathbf{V}_o^{oc} (\mathbf{V}_o^{oc})^H > = < a_o^2 > < \mathbf{V}_o^{oc} (\mathbf{V}_o^{oc})^H > \quad \text{(A6)}$$

(assuming magnitudes of narrowband signals are uncorrelated to the angles of arrivals)

Also, assuming the interfering signals are uncorrelated with the desired signal, then $<a_o a_k> = <a_o> <a_k> = 0$

since the phase $\beta_o$ is assumed uniform over $(0, 2\pi)$. So

$$< a_o a_k e^{j(\beta k - \beta o)} \mathbf{V}_k^{oc} (\mathbf{V}_o^{oc})^H > = <a_o> <a_k> <e^{j\beta k} > < e^{j\beta o}> <\mathbf{V}_k^{oc}><\mathbf{V}_o^{oc\,H}> \quad \text{(A7)}$$

$$= 0$$

and $< a_k a_l e^{j(\beta k - \beta l)} \mathbf{V}_k^{oc} (\mathbf{V}_l^{oc})^H > = \delta_{kl} < a_k^2 \mathbf{V}_k^{oc} (\mathbf{V}_k^{oc})^H >$

$$= \delta_{kl} < a_k^2 > <\mathbf{V}_k^{oc} (\mathbf{V}_k^{oc})^H > \quad \text{(A8)}$$

Now consider $<\mathbf{V}_k^{oc} (\mathbf{V}_k^{oc})^H > = V_o^2 < e^{jk_o d(m-n)\cos\phi_k} >$

$$= V_o^2 < e^{jk_o d(m-n)\{\cos\bar{\phi}_k \cos\alpha_k - \sin\bar{\phi}_k \sin\alpha_k\}} >$$

$$= V_o^2 < e^{j\frac{k_o d(m-n)}{b_k}\{\cos\bar{\phi}_k\sqrt{b_k^2-\tau^2} - \sin\bar{\phi}_k\tau\}} >$$

where $\tau = \dfrac{R_k}{r_k}\sin\alpha_k$ (A9)

$$= V_o^2 \int_{-1}^{1} e^{j\frac{k_o d(m-n)}{b_k}\{\cos\bar{\phi}_k\sqrt{b_k^2-\tau^2} - \sin\bar{\phi}_k\tau\}} \frac{2}{\pi}\sqrt{1-\tau^2}\,d\tau$$

$$= V_o^2 \int_{-1}^{1} \cos\left(\frac{k_o d(m-n)}{b_k}\tau\sin\bar{\phi}_k\right) e^{j\frac{k_o d(m-n)}{b_k}\cos\bar{\phi}_k\sqrt{b_k^2-\tau^2}} \frac{2}{\pi}\sqrt{1-\tau^2}\,d\tau$$

Let us now assume that $b_k >> \sqrt{10} \Rightarrow b_k^2 >> 10$, so that $\sqrt{b_k^2 - \tau^2} \approx b_k$, then

$$<\mathbf{V_k^{oc}}(\mathbf{V_k^{oc}})^{\mathbf{H}}> \approx V_o^2 e^{jk_o d(m-n)\cos\bar{\phi}_k} \frac{2}{\pi}\int_{-1}^{1}\sqrt{1-\tau^2}\cos\left(\frac{k_o d(m-n)r_k}{R_k}\tau\sin\bar{\phi}_k\right)d\tau$$

$$= V_o^2 e^{jk_o d(m-n)\cos\bar{\phi}_k} \frac{2J_1\left[(k_o d(m-n)\sin\bar{\phi}_k \frac{r_k}{R_k})\right]}{\left[(k_o d(m-n)\sin\bar{\phi}_k \frac{r_k}{R_k})\right]}$$

$$= V_o^2 e^{jk_o d(m-n)\cos\bar{\phi}_k} f_{m-n}(k_o d\sin\bar{\phi}_k, r_k, R_k) \qquad \text{(A10)}$$

where $f_{m-n}(k_o d\sin\bar{\phi}_k, r_k, R_k) = \dfrac{2J_1\left(\dfrac{k_o d(m-n)\sin\bar{\phi}_k r_k}{R_k}\right)}{\dfrac{k_o d(m-n)\sin\bar{\phi}_k r_k}{R_k}}$ (A11)

and $J_1$ = Bessel's function of the 1st kind, of order 1.

Substituting (A9) into (A4),

$$< \mathbf{V_t^{oc}}\,\mathbf{V_t^{oc\,H}} >_{mn} = V_o^2 \{ <a_o^2> e^{jk_o d(m-n)\cos\bar{\phi}_o} f_{m-n}(k_o d\sin\bar{\phi}_o, r_o, R_o)$$

$$+ \Sigma <a_k^2> e^{jk_o d(m-n)\cos\bar{\phi}_k} f_{m-n}(k_o d\sin\bar{\phi}_k, r_k, R_k) \}$$

Therefore, $< \mathbf{V_t^{oc}}\,\mathbf{V_t^{oc\,H}} > = V_o^2 \{ <a_o^2> \mathbf{C_o} + \Sigma (<a_k^2> \mathbf{C_k}) \}$ (A12)

where $[C_k]_{mn} = e^{jk_o d(m-n)\cos\bar{\phi}_k} \dfrac{2J_1\left(\dfrac{k_o d(m-n)\sin\bar{\phi}_k r_k}{R_k}\right)}{\dfrac{k_o d(m-n)\sin\bar{\phi}_k r_k}{R_k}}$ (A13)

Finally, $\Phi = \mathbf{Z_c} < \mathbf{V_t^{oc}}\,\mathbf{V_t^{oc\,H}} > \mathbf{Z_c^H} + < \mathbf{N}\,\mathbf{V_t^{oc\,H}} > \mathbf{Z_c^H} + \mathbf{Z_c} < \mathbf{V_t^{oc}}\,\mathbf{N^H} > + < \mathbf{N}\,\mathbf{N^H} >$

$= V_o^2 + V_o^2 \mathbf{Z_c} \{ <a_o^2> \mathbf{C_o} + \Sigma (<a_k^2> \mathbf{C_k}) \} \mathbf{Z_c^H}$

$= \tilde{V}_N^2 + \tilde{V}_N^2 \mathbf{Z_c} (\xi_o \mathbf{C_o}) \mathbf{Z_c^H} + \tilde{V}_N^2 \mathbf{Z_c} (\Sigma \xi_k \mathbf{C_k}) \mathbf{Z_c^H}$

$= \tilde{V}_N^2 [ \mathbf{U} + \mathbf{Z_c} (\xi_o \mathbf{C_o}) \mathbf{Z_c^H} + \mathbf{Z_c} (\Sigma \xi_k \mathbf{C_k}) \mathbf{Z_c^H} ]$ (A14)

where $\xi_o = \dfrac{V_o^2 < a_o^2 >}{V_N^2}$ is the input signal to thermal noise ratio (A15)

$\xi_k = \dfrac{V_o^2 < a_k^2 >}{V_N^2}$ is the input interference to thermal noise ratio (A16)

B. EXPRESSION FOR S

From (16) $\mathbf{S} = <\mathbf{A_r^H}\,\mathbf{V_t}>$

where $\mathbf{A_r}$ (reference signal) takes the form $a_o V_o e^{j(\omega_o t+\beta_o)}$ (A17)

then $\mathbf{S} = < a_o V_o e^{-j(\omega_o t+\beta_o)} \{ \mathbf{Z_c} [a_o e^{j(\omega_o t+\beta_o)}\, V_o^{oc} + \sum_{1}^{K} a_k e^{j(\omega_o t+\beta_k)} V_k^{oc} ] + \mathbf{N}(t) \} >$

$= V_o \mathbf{Z_c} < a_o^2 (\mathbf{V_o^{oc}}) + \Sigma (a_o a_k e^{j(\beta k - \beta o)}\, \mathbf{V_k^{oc}}) >$ (A18)

$+ V_o < a_o e^{-j(\omega_o t+\beta_o)} \mathbf{N}(t) >$

$< \mathbf{V_o^{oc}} >_n = V_o < e^{jk_o d(n-1)\cos\phi_o} >$

$$\approx V_o \; e^{jk_o d(n-1)\cos\bar{\phi}_o} f_{n-1}(k_o d \sin\bar{\phi}_o, r_o, R \;) \qquad \text{(A19)}$$

Lastly, $< a_o \, a_k \, e^{j(\beta k - \beta o)} \, \mathbf{V_k}^{oc} > \; = < a_o \, a_k > < e^{j(\beta k - \beta o)} > < \mathbf{V_k}^{oc} > = 0 \qquad \text{(A20)}$

where $< a_o \, a_k > = 0$.

Therefore, using (A20), (A23) and (A24),

$$\mathbf{S} \quad = V_o^{\,2} < a_o^{\,2} > \mathbf{Z_c} \, [ \, f_{n-1}(k_o d, \, r_o, \, R_o) \, ]$$

$$= \tilde{V}_N^2 \; \xi_o \, \mathbf{Z_c} \, \mathbf{C_s} \qquad \text{(A21)}$$

where

$$[C_s]_m = e^{jk_o d(m-1)\cos\bar{\phi}_o} \; \frac{2J_1(k_o d(m-1)\sin\bar{\phi}_o \, \frac{r_o}{R_o})}{(k_o d(m-1)\sin\bar{\phi}_o \, \frac{r_o}{R_o})} \qquad \text{(A22)}$$

# APPENDIX B : EXPRESSIONS FOR $P_o$ AND $P_k$

From (32), we have

$$P_o = < (\mathbf{w}^H \mathbf{Z}_c \mathbf{A}_o \mathbf{V}_o^{oc}) (\mathbf{w}^H \mathbf{Z}_c \mathbf{A}_o \mathbf{V}_o^{oc})^H >$$

$$= <a_o^2> \mathbf{w}^H \mathbf{Z}_c <\mathbf{V}_o^{oc} \mathbf{V}_o^{oc\,H}> \mathbf{Z}_c^H \mathbf{w}$$

$$= \tilde{V}_N^2 \, \xi_o \, \mathbf{w}^H \mathbf{Z}_c \mathbf{C}_o \mathbf{Z}_c^H \mathbf{w} \qquad \text{(B1)}$$

From (33), we have

$$P_k = < (\mathbf{w}^H \mathbf{Z}_c \mathbf{A}_k \mathbf{V}_k^{oc}) (\mathbf{w}^H \mathbf{Z}_c \mathbf{A}_k \mathbf{V}_k^{oc})^H >$$

$$= <a_k^2> \mathbf{w}^H \mathbf{Z}_c <\mathbf{V}_k^{oc} \mathbf{V}_k^{oc\,H}> \mathbf{Z}_c^H \mathbf{w}$$

$$= \tilde{V}_N^2 \, \mathbf{w}^H \mathbf{Z}_c (\Sigma \xi_k \mathbf{C}_k) \mathbf{Z}_c^H \mathbf{w} \qquad \text{(B2)}$$

where $V_N$ = root mean square noise voltage

$\xi_o$ , $\xi_k$ as defined in (A16) and (A17)

# LIST OF REFERENCES


1. Applebaum, S.P., "Adaptive Arrays," *IEEE Trans. Antennas Propag*, Vol 24, September 1976.

2. Eggers, P.C.E., "Generation of Base Station DOA Distribution via Jacobi Transformation of Scattering Areas," *Electronics Letters*, 34(1), January 1998.

3. Childers, D.G., *Probability and Random Processes*, WCB McGraw-Hill, 1997.

4. Janaswamy, R., "*Unpublished Notes,*" Naval Postgraduate School, Monterey, CA, January 1999.

5. Kraus, J.D., *Antennas*, McGraw-Hill, 1950.

6. Litva, J. and Lo, T. K-Y., *Digital Beamforming in Wireless Communications*, Artech House, 1996.

7. Vaughan, R. and Andersen, J., "Antenna Diversity in Mobile Communications," *IEEE Trans. On Vehicular Technology*, Vol 36, No. 4 November 1987.

8. Gupta, I.J. and Ksienski, A.A., "Effect of Mutual Coupling on the Performance of Adaptive Arrays," *IEEE Trans. Antennas Propag*, Vol 31, September 1983.

9. Parsons, D., *The Mobile Radio Propagation Channel*, Pentech Press, 1992.

10. Stutzman, W.L. and Thiele, G.A., *Antenna Theory and Design*, John Wiley and Sons, 1981.

11. Collin, R.E., *Antennas and Radiowave Propagation*, McGraw-Hill, 1985.

12. Steyskal, H. and Herd, J., "Mutual Coupling Compensations in Small Order Antennas," *IEEE Trans. Antennas Propag*, Vol 38 December 1990.

13. Kang, Y-W. and Pozar, D., "Correction of Error in Reduced Sidelobe Synthesis due to Mutual Coupling," *IEEE Trans. Antennas Propag*, Vol AP – 38, December 1985.

14. Monzingo, R.A. and Miller, T.W., *Introduction to Adaptive Arrays*, John Wiley and Sons, 1980.

# INITIAL DISTRIBUTION LIST

1. Defense Technical Information Center .....2
   8725 John J. Kingman Rd., STE 0944
   Ft Belvoir, VA 22060 – 6218

2. Dudley Knox Library .....2
   Naval Postgraduate School
   411 Dyer Rd.
   Monterey CA 93943 – 5101

3. Chairman, Code IW.....1
   Information Warfare Academic Group
   Naval Postgraduate School
   Monterey, CA 93943

4. Professor Rama Janaswamy, Code EC/ JS .....1
   Department of Electrical and Computer Engineering
   Naval Postgraduate School
   Monterey CA 93943

5. Dr David Jenn, Code EC/JN.....1
   Department of Electrical and Computer Engineering
   Naval Postgraduate School
   Monterey CA 93943

6. Professor J.B. Andersen .....1
   Center for Personkommunikation, AAU
   Fredrik Bajers Vej 7A-5
   9220 Aalborg, Denmark

7. Professor E. Bonek .....1
   Institut fuer Nachrichtentechnik Und Hockfrequenztechnik
   Technische Universitaet Wien
   Gusshaustrasse 25/389
   A-1040 Wien, Austria

8. MAJ Tan Hong Wee.....1
   HQ - RSN
   Ministry of Defence
   303 Gombak Drive
   S669645
   Republic of Singapore

66 553NPS TH 3791
11/99 22527-106 MULE

DUDLEY KNOX LIBRARY
3 2768 00366454 1